Title: Toward realization of novel superconductivity based on twisted van der Waals Josephson junction in Cuprates

Speakers: Philip Kim

Series: Quantum Matter

Date: February 28, 2022 - 12:00 PM

URL: https://pirsa.org/22020071

Abstract: Twisted interfaces between stacked van der Waals Cuprate crystals enable tunable Josephson coupling, utilizing anisotropic superconducting order parameters. Employing a novel cryogenic assembly technique, we fabricate high-temperature Josephson junctions with an atomically sharp twisted interface between Bi_2Sr_2CaCu_2O_{8+x} crystals. The critical current density J_c sensitively depends on the twist angle. While near 0 degree twist, J_c nearly matches that of intrinsic junctions, it is suppressed almost 2-orders of magnitude but remained finite near 45 degree. J_c also exhibits non-monotonic behavior versus temperature due to competition between two supercurrent contributions from nodal and anti-nodal regions of the Fermi surface. Near 45 degree twist angle, we observe two-period Fraunhofer interference patterns and fractional Shapiro steps at half integer values, a signature of co-tunneling Cooper pairs necessary for high temperature topological superconductivity.

Zoom Link: https://pitp.zoom.us/meeting/register/tJcqc-ihqzMvHdW-YBm7mYd_XP9Amhypv5vO

Toward realization of novel superconductivity based on twisted van der Waals Josephson junction in cuprates

Philip Kim

Department of Physics, Harvard University

Acknowledgment

Experiment

Frank Zhao, Nicolar Poccia, Xiaomeng Cui, Hyobin Yoo, Joon Young Park, Yuval Ronen, Rebecca Engelke

TEM

Joules Gardener, Austin Akey (CNS); Sangmin Lee, Miyoung Kim (SNU)

Samples

Rudan Zhong, Genda Gu (BNL); Kenji Watanabe, Takashi Taniguchi (NIMS)

Theory

Pavel Volkov, Jed Pixley (Rutgers); Tarun Tummuru, Stephan Plugge, Marcel Franz (UBC)

NSF

Office of Naval Research

Moire Superlattice Engineering in van der Waals Interface

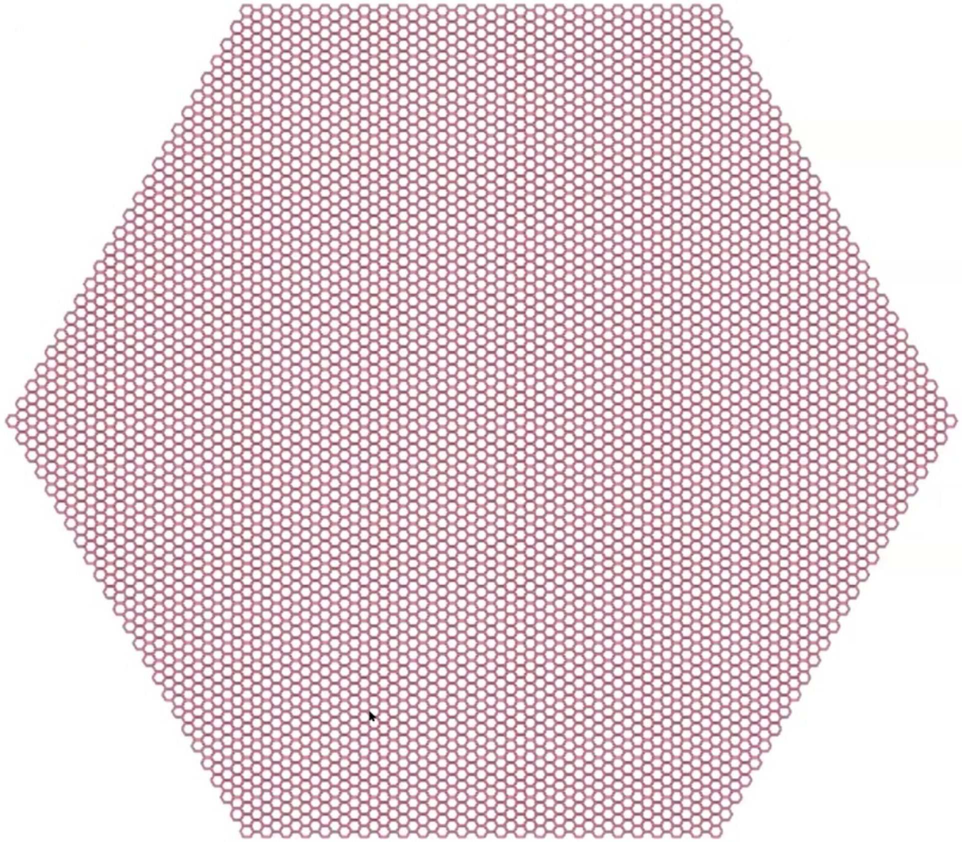

Twisted van der Waal interface of homo & hetero structure

Animation from Jarillo-Herrero group

Moire Superlattice Engineering in van der Waals Interface

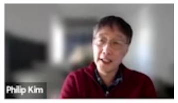

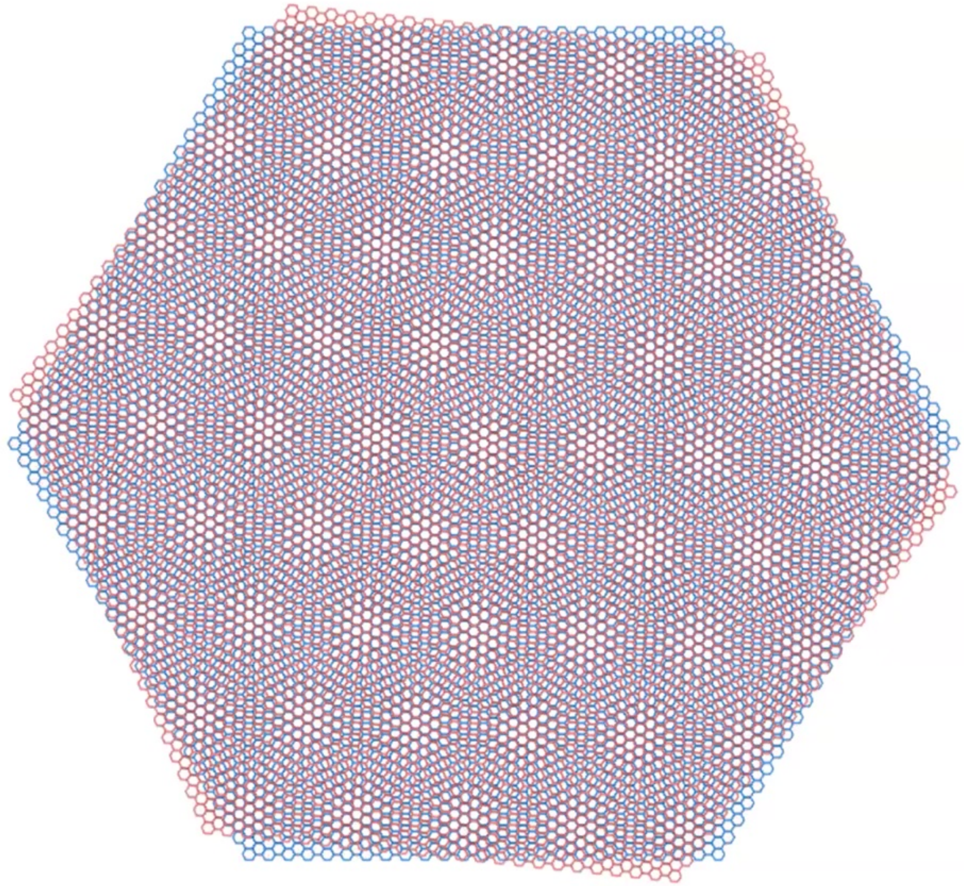

Twisted van der Waal interface of homo & hetero structure

Animation from Jarillo-Herrero group

Moire Superlattice Engineering in van der Waals Interface

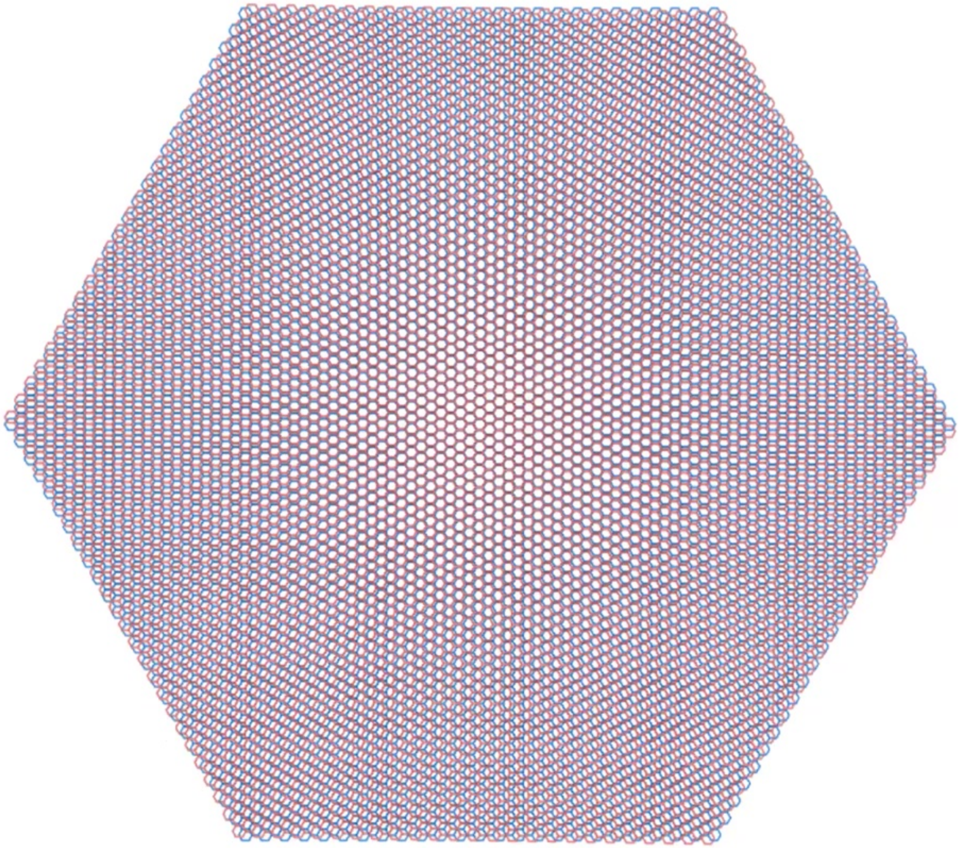

Twisted van der Waal interface of homo & hetero structure

Animation from Jarillo-Herrero group

Moire Superlattice Engineering in van der Waals Interface

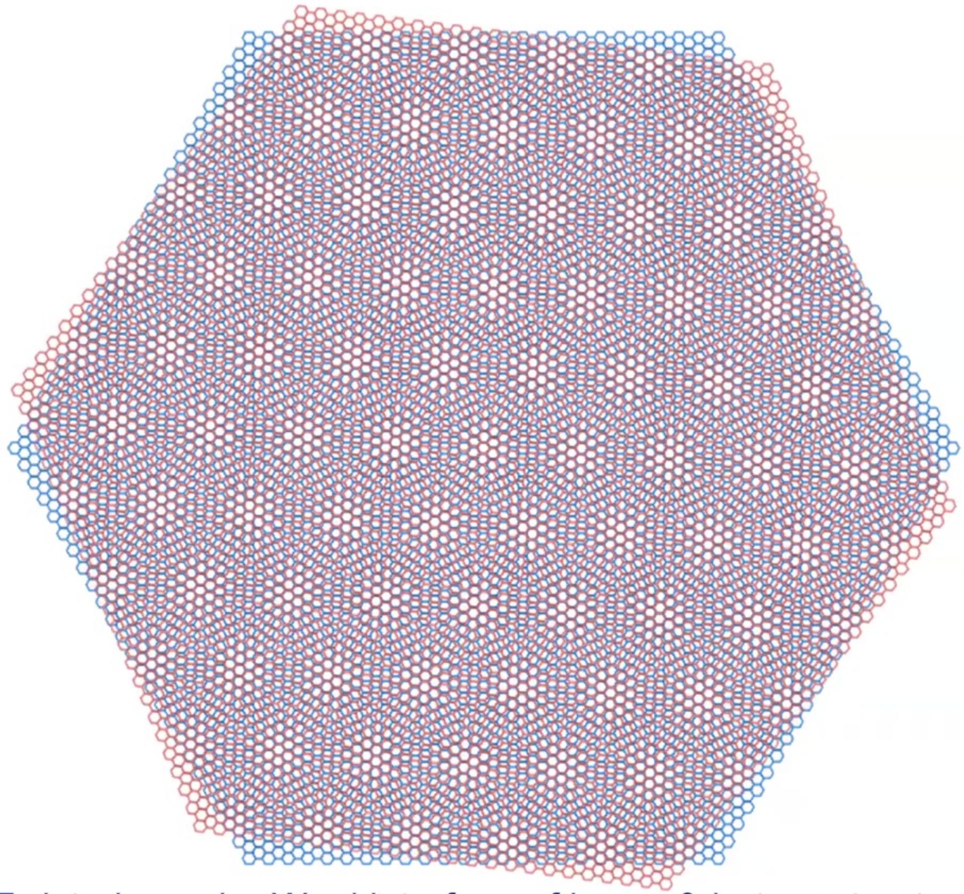

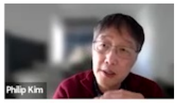

Twisted van der Waal interface of homo & hetero structure

Animation from Jarillo-Herrero group

Correlated Quantum State in Twisted Graphene Bilayer

ARTICLE

5 APRIL 2018 | VOL 556 | NATURE | 43

doi:10.1038/nature26160

Unconventional superconductivity in magic-angle graphene superlattices

Yuan Cao[1], Valla Fatemi[1], Shiang Fang[2], Kenji Watanabe[3], Takashi Taniguchi[3], Efthimios Kaxiras[2,4] & Pablo Jarillo-Herrero[1]

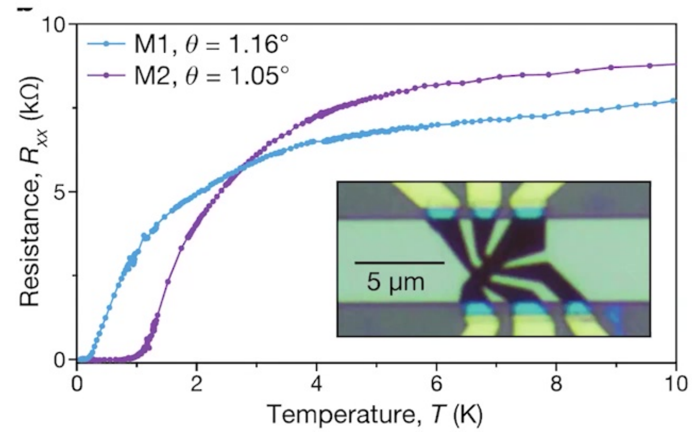

Correlated insulator
Cao et al., Nature 556, 80–84 (2018).
Burg et al., PRL 123, 197702 (2019).

Unconventional superconductivity
Cao et al., Nature 556, 43–50 (2018).
Yankowitz el al, Science 363, 1059–1064 (2019).
Lu et al, Nature 574, 653–657 (2019).

Magnetism and Quantum Anomalous Hall Effect
Sharpe et al., Science 365, 605–608 (2019).
Serlin et al., arXiv:1907.00261 (2019).

Trilayers double bilayers
Chen et al. Nature Physics 15, 237–241 (2019).
Chen et al., Nature 572, 215219 (2019).She et al., ArXiv 2019

Double bilayers
Shen et al., arXiv:1903.06952 (2019).
Liu et al, arXiv:1903.08130 (2019).
Cao et al., arXiv:1903.08596 (2019).
Adak et al., arXiv:2001.09916 (2020)

TMDC/TMDC; TMDC/TBG
Tang et al. arXiv:1910.08673 (2019).
Regan et al., arXiv:1910.09047 (2019).
Wang et al., arXiv:1910.12147 (2019).
Arora et al., Nature 583, 379 (2020)
***

$Bi_2Sr_2CaCu_2O_{8+x}$: A Cuprate van der Waals Material

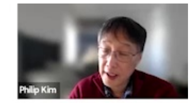

N. Poccia et al. Phys. Rev. Mater. **4**, 114007 (2020)

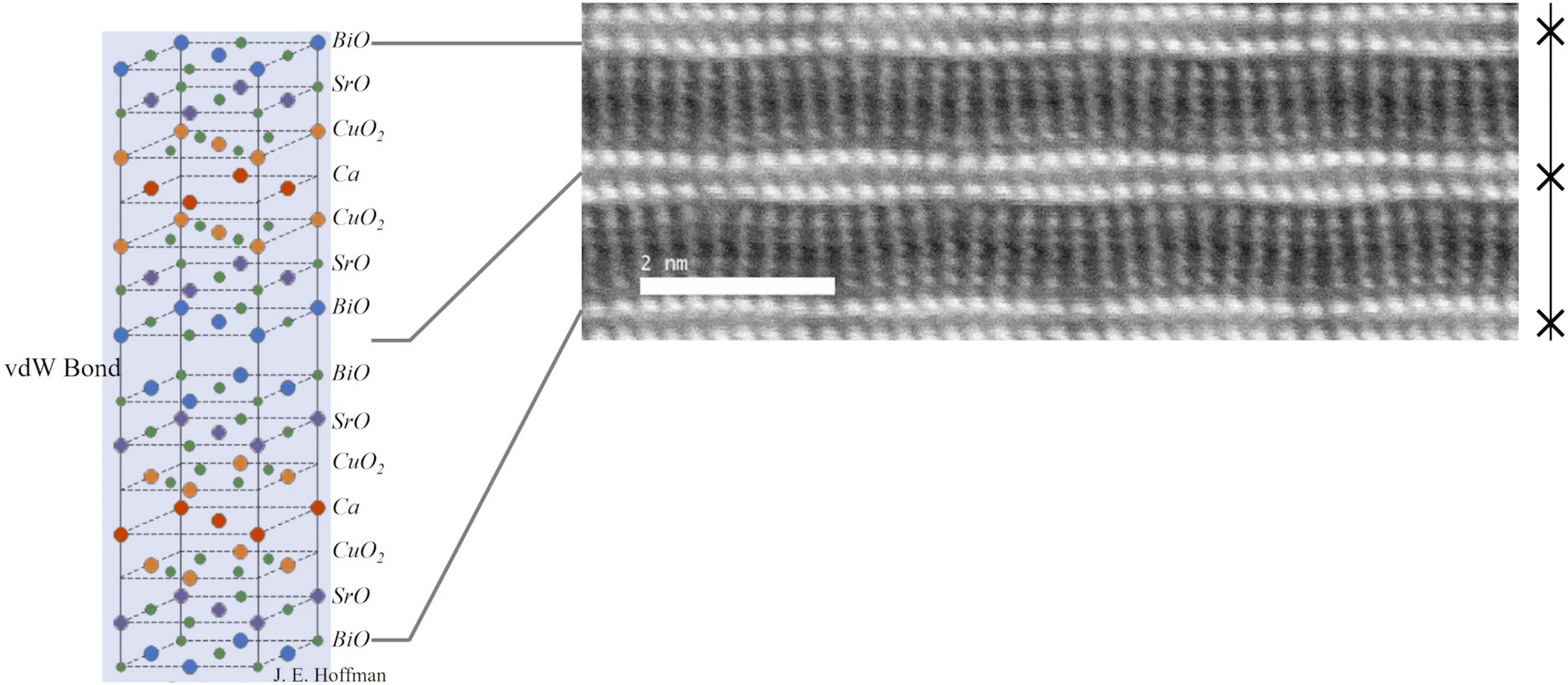

$Bi_2Sr_2CaCu_2O_{8+x}$: A Cuprate van der Waals Material

N. Poccia et al. Phys. Rev. Mater. **4**, 114007 (2020)

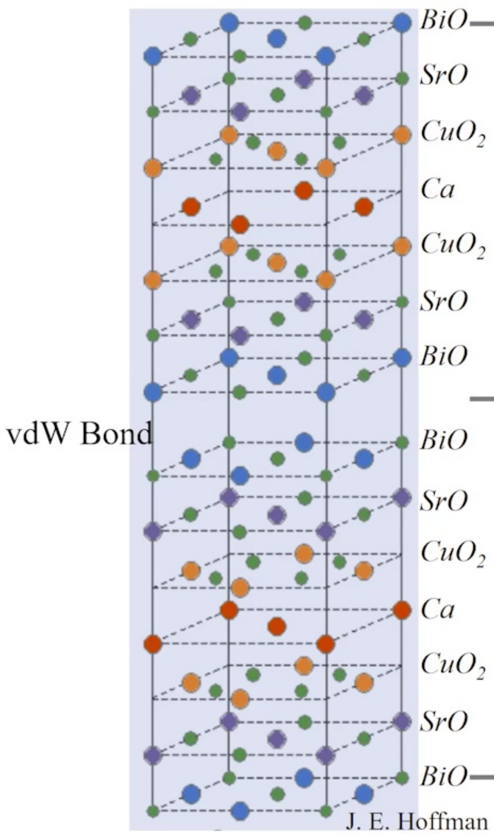

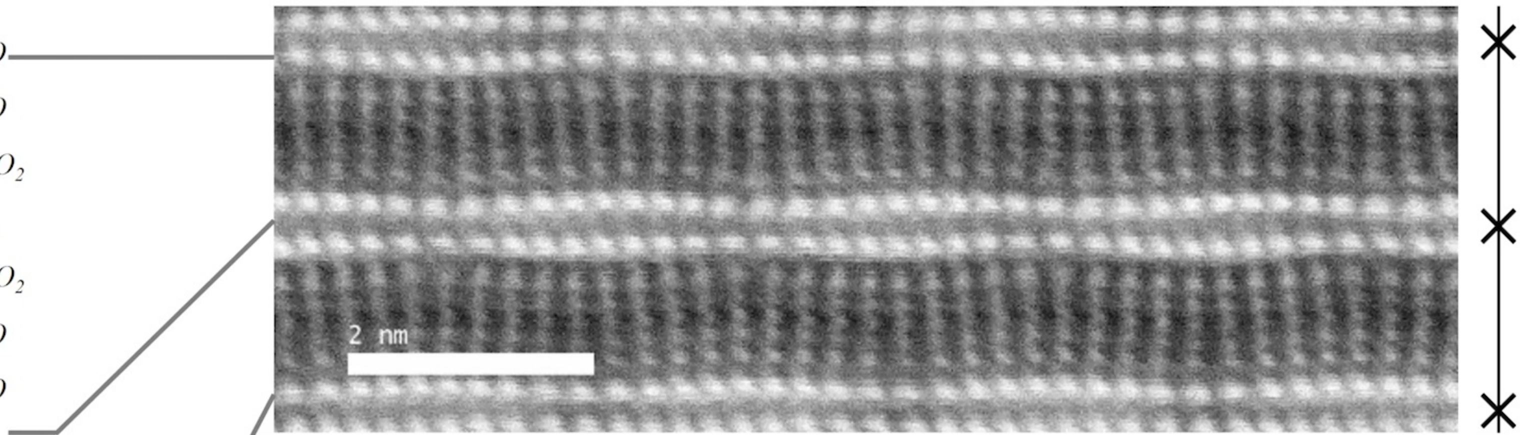

Superconducting down to a half unit cell!

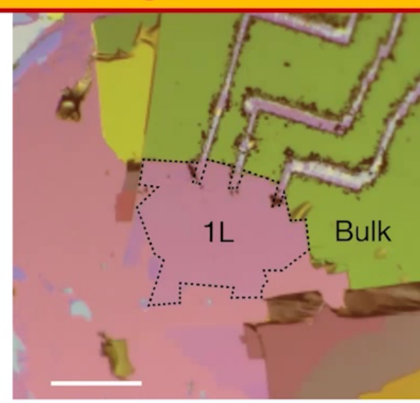

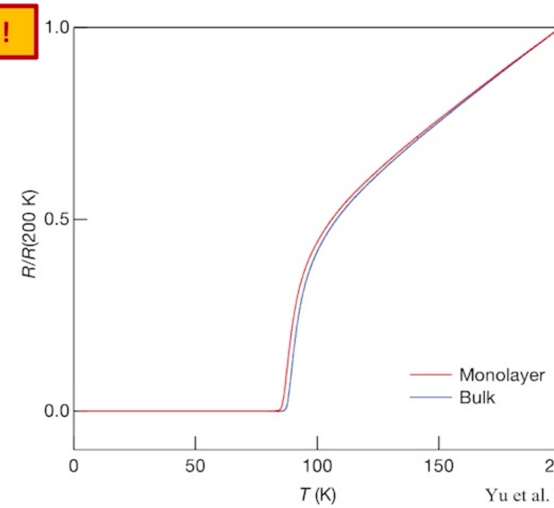

Yu et al. Nature 575, 156 (2019)

Twisted Cuprate Junctions

nature physics

ARTICLES

https://doi.org/10.1038/s41567-020-01142-7

Check for updates

High-temperature topological superconductivity in twisted double-layer copper oxides

Oguzhan Can[1,2], Tarun Tummuru[1,2], Ryan P. Day[1,2], Ilya Elfimov[1,2], Andrea Damascelli[1,2] and Marcel Franz[1,2] ✉

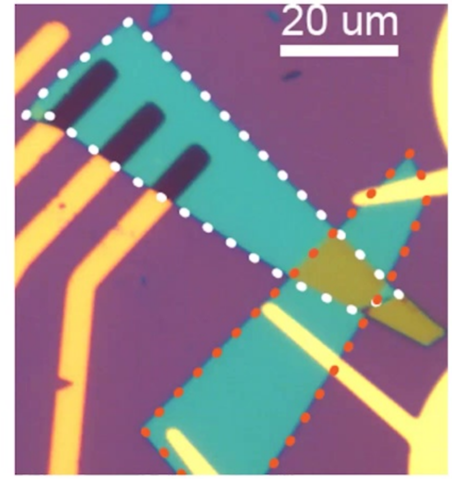

S. Y. F Zhao et al., arXiv 2108.13455

Magic angles and current-induced topology in twisted nodal superconductors

Pavel A. Volkov,* Justin H. Wilson, and J. H. Pixley
Department of Physics and Astronomy, Center for Materials Theory, Rutgers University, Piscataway, NJ 08854, USA
(Dated: December 16, 2020)

Nodal d-wave Superconductor

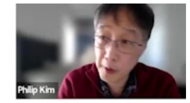

Cuprate Brillouin Zone

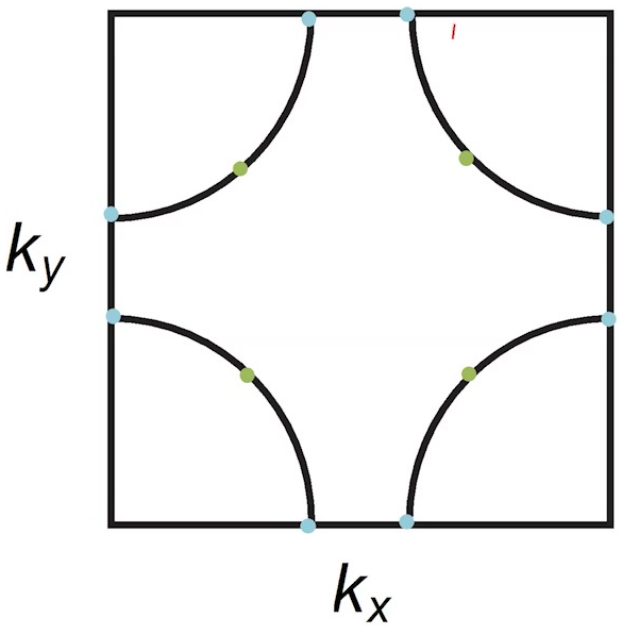

D-wave order parameter

$$\Delta_k = \Delta_0(\cos k_x - \cos k_y)$$

BdG Hamiltonian:

$$\hat{H} = \sum_{\mathbf{k}} \begin{pmatrix} c_\uparrow(\mathbf{k}) \\ c_\downarrow^\dagger(\mathbf{k}) \end{pmatrix}^\dagger \begin{pmatrix} \varepsilon(\mathbf{k}) & \Delta(\mathbf{k}) \\ \Delta^*(\mathbf{k}) & -\varepsilon(\mathbf{k}) \end{pmatrix} \begin{pmatrix} c_\uparrow(\mathbf{k}) \\ c_\downarrow^\dagger(\mathbf{k}) \end{pmatrix}$$

$$\approx \sum_{\mathbf{k}} \begin{pmatrix} c_\uparrow(\mathbf{k}) \\ c_\downarrow^\dagger(\mathbf{k}) \end{pmatrix}^\dagger \begin{pmatrix} \mathbf{v}_F \cdot \mathbf{p} & \mathbf{v}_\Delta \cdot \mathbf{p} \\ \mathbf{v}_\Delta \cdot \mathbf{p} & -\mathbf{v}_F \cdot \mathbf{p} \end{pmatrix} \begin{pmatrix} c_\uparrow(\mathbf{k}) \\ c_\downarrow^\dagger(\mathbf{k}) \end{pmatrix}$$

near the nodal points

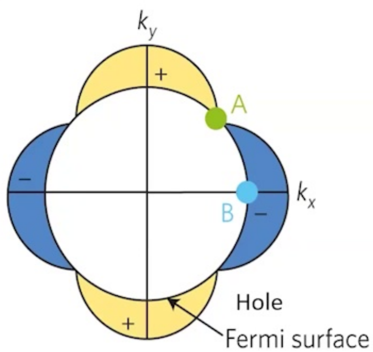

Gap vanishes at the nodal points

Nodal d-wave Superconductor

Cuprate Brillouin Zone

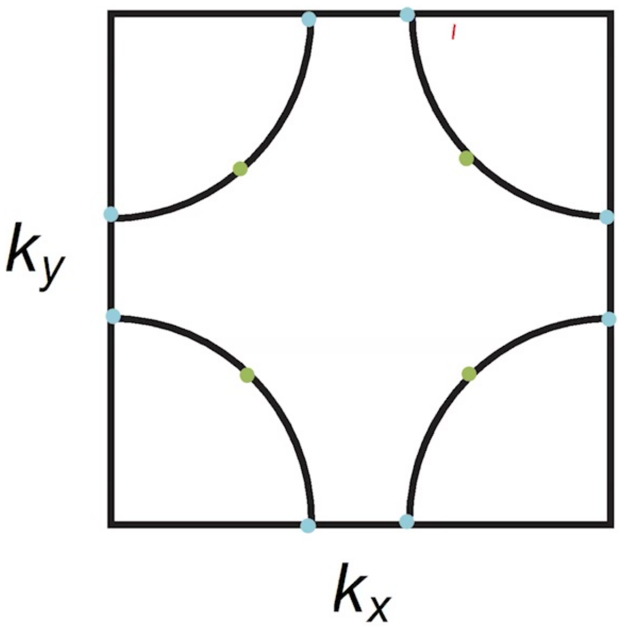

D-wave order parameter

$$\Delta_k = \Delta_0(\cos k_x - \cos k_y)$$

BdG Hamiltonian:

$$\hat{H} = \sum_{\mathbf{k}} \begin{pmatrix} c_\uparrow(\mathbf{k}) \\ c_\downarrow^\dagger(\mathbf{k}) \end{pmatrix}^\dagger \begin{pmatrix} \varepsilon(\mathbf{k}) & \Delta(\mathbf{k}) \\ \Delta^*(\mathbf{k}) & -\varepsilon(\mathbf{k}) \end{pmatrix} \begin{pmatrix} c_\uparrow(\mathbf{k}) \\ c_\downarrow^\dagger(\mathbf{k}) \end{pmatrix}$$

$$\approx \sum_{\mathbf{k}} \begin{pmatrix} c_\uparrow(\mathbf{k}) \\ c_\downarrow^\dagger(\mathbf{k}) \end{pmatrix}^\dagger \begin{pmatrix} \mathbf{v}_F \cdot \mathbf{p} & \mathbf{v}_\Delta \cdot \mathbf{p} \\ \mathbf{v}_\Delta \cdot \mathbf{p} & -\mathbf{v}_F \cdot \mathbf{p} \end{pmatrix} \begin{pmatrix} c_\uparrow(\mathbf{k}) \\ c_\downarrow^\dagger(\mathbf{k}) \end{pmatrix}$$

near the nodal points

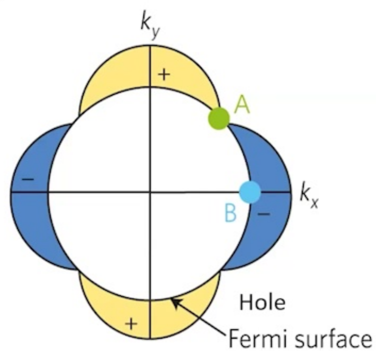

$$E_{0,\pm}(\mathbf{k}) = \pm\sqrt{v_F^2 k_\parallel^2 + v_\Delta^2 k_\perp^2}$$

Gap vanishes at the nodal points

Twisted Cuprate Junction

Stacked twist layer

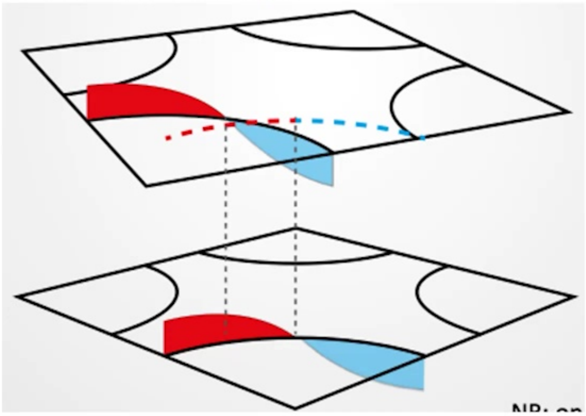

Volkov et al. arXiv: 2012.07860

Double layer Nambu basis

$$\Psi_{\mathbf{k}} = (c_{\mathbf{k}\uparrow 1}, c^{\dagger}_{-\mathbf{k}\downarrow 1}, c_{\mathbf{k}\uparrow 2}, c^{\dagger}_{-\mathbf{k}\downarrow 2})^{T}$$

BdG Hamiltonian

$$\mathcal{H} = \sum_{\mathbf{k}} \Psi^{\dagger}_{\mathbf{k}} h_{\mathbf{k}} \Psi_{\mathbf{k}} + E_0.$$

layer1   Interlayer coupling

$$h_{\mathbf{k}} = \begin{pmatrix} \xi_{\mathbf{k}} & \Delta_{\mathbf{k}1} & g & 0 \\ \Delta^{*}_{\mathbf{k}1} & -\xi_{\mathbf{k}} & 0 & -g \\ g & 0 & \xi_{\mathbf{k}} & \Delta_{\mathbf{k}2} \\ 0 & -g & \Delta^{*}_{\mathbf{k}2} & -\xi_{\mathbf{k}} \end{pmatrix}$$

layer2

Small twist angle   **Large twist angle**

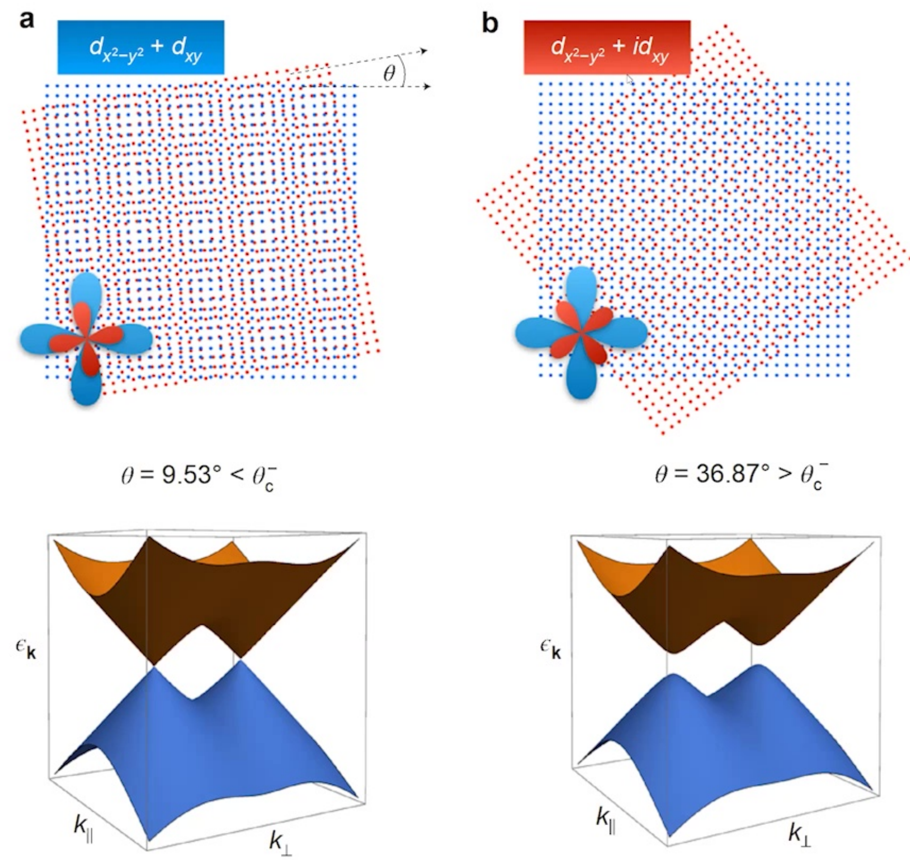

Can et al. Nature Phys (2021)

Twisted Cuprate Junction

Stacked twist layer

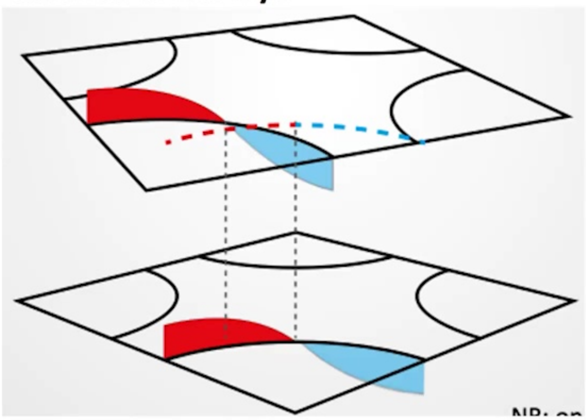

Volkov et al. arXiv: 2012.07860

Double layer Nambu basis

$$\Psi_{\mathbf{k}} = (c_{\mathbf{k}\uparrow 1}, c^{\dagger}_{-\mathbf{k}\downarrow 1}, c_{\mathbf{k}\uparrow 2}, c^{\dagger}_{-\mathbf{k}\downarrow 2})^T$$

BdG Hamiltonian

$$\mathcal{H} = \sum_{\mathbf{k}} \Psi^{\dagger}_{\mathbf{k}} h_{\mathbf{k}} \Psi_{\mathbf{k}} + E_0.$$

layer1 Interlayer coupling

$$h_{\mathbf{k}} = \begin{pmatrix} \xi_{\mathbf{k}} & \Delta_{\mathbf{k}1} & g & 0 \\ \Delta^*_{\mathbf{k}1} & -\xi_{\mathbf{k}} & 0 & -g \\ g & 0 & \xi_{\mathbf{k}} & \Delta_{\mathbf{k}2} \\ 0 & -g & \Delta^*_{\mathbf{k}2} & -\xi_{\mathbf{k}} \end{pmatrix}$$

layer2

SC with broken TRS

Small twist angle | **Large twist angle**

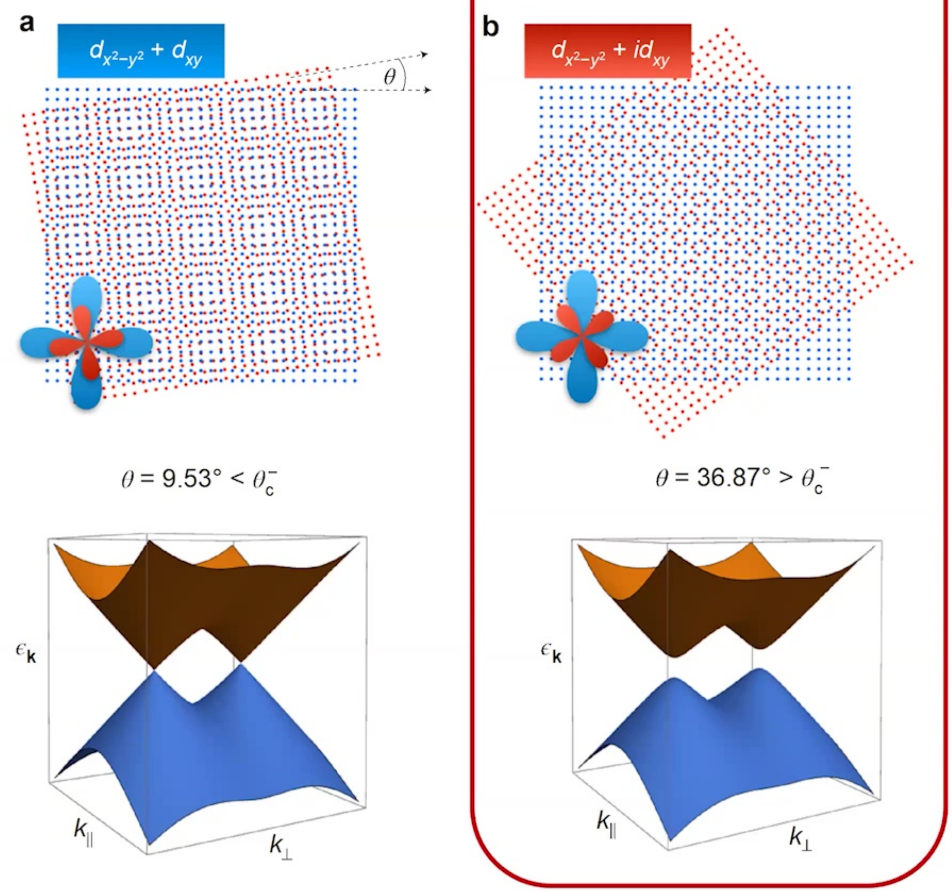

Can et al. Nature Phys (2021)

45° Twisted Junction: Superconductivity with Broken TRS

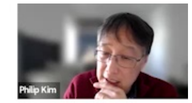

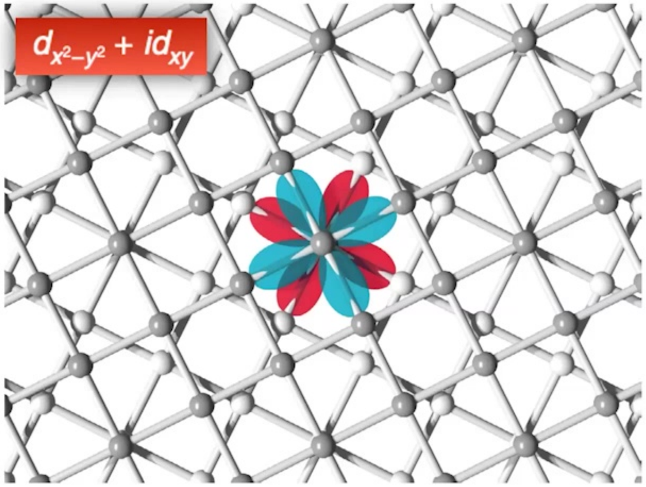

BdG Free Energy

$$\mathcal{F}(\varphi) = E_0 - 2k_B T \sum_{k,a=\pm} \ln[2\cosh[E_{ka}(\varphi)/2k_B T]]$$

Ginzburg Landau Free Energy

$$\mathcal{F}(\varphi) = \mathcal{F}_0 + 2B_0\psi^2[-\cos(2\theta)\cos\varphi + \mathcal{K}\cos(2\varphi)]$$

Phase diff. between SCs

Twisted angle

No nodal points: bulk has SC gap always!

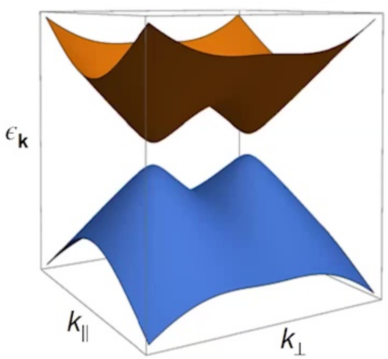

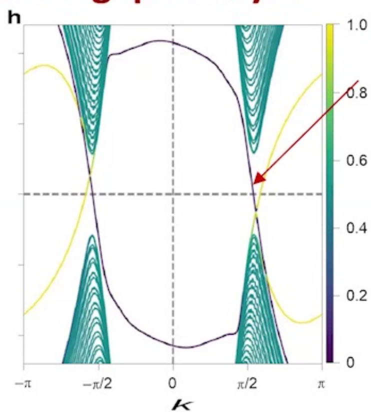

BdG spectrum of stripe SC

Topological edge states in the gap may appear depending the coupling parameters

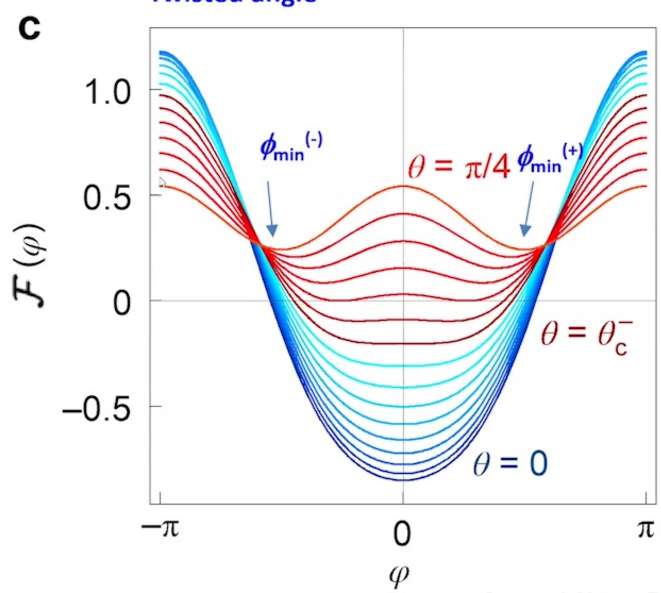

Can et al. Nature Phys (2021)

Experiments on Twist Cuprate Josephson Junctions

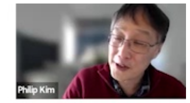

Bulk Crystals
30 hrs
'below melting temperature'

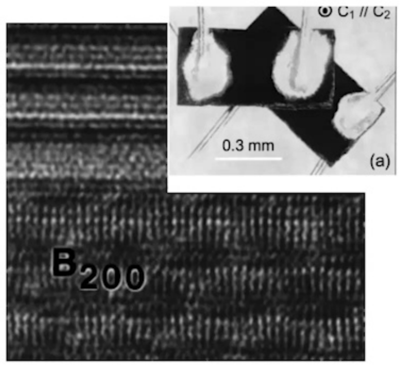

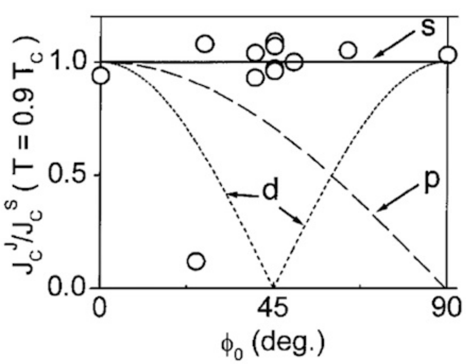

Li et al, PRL 83, 4160 (1999); Zhu et al PRB 57 8601 (1998)

Artificial Whisker Junctions
30 min
850 °C

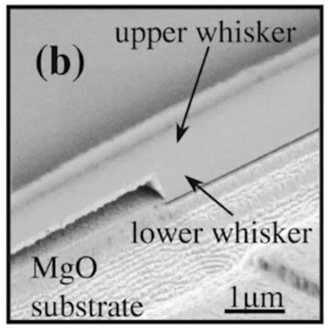

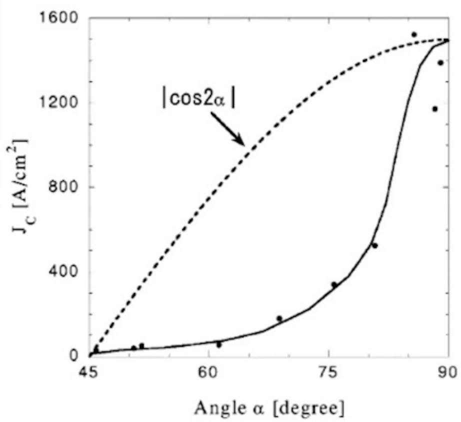

Takano et al, PRB 65, 140513 (2002)

Natural Whisker Junctions
20 min
845 °C

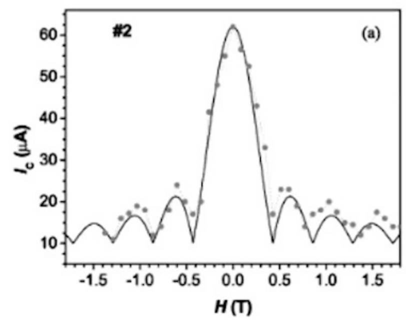

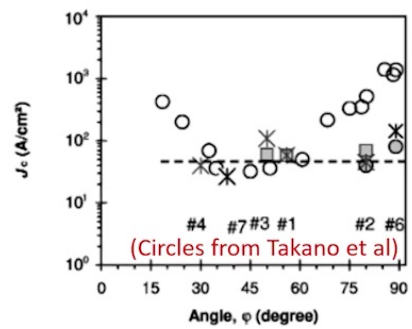

Latyshev et al, PRB 70, 094517 (2004)

Exfoliated Flakes
10 min
450-530 °C

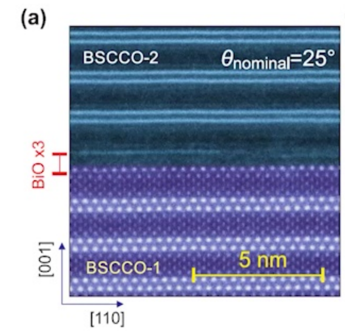

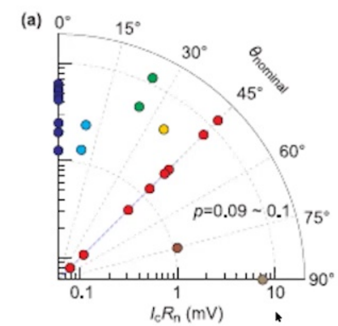

Zhu et al, ArXiv 1903.07965 (2021)

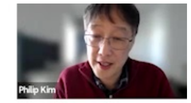

Fab in a Glovebox UHV

- *Stacking*
- *Selection*
- ✓ *Deposition*
- ✓ *Etch*
- ✓ *Packaging*

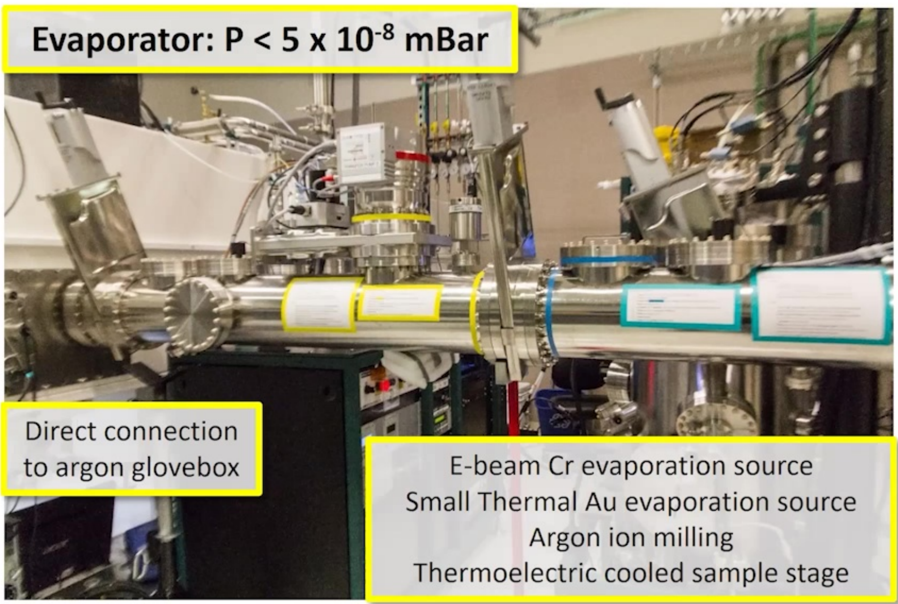

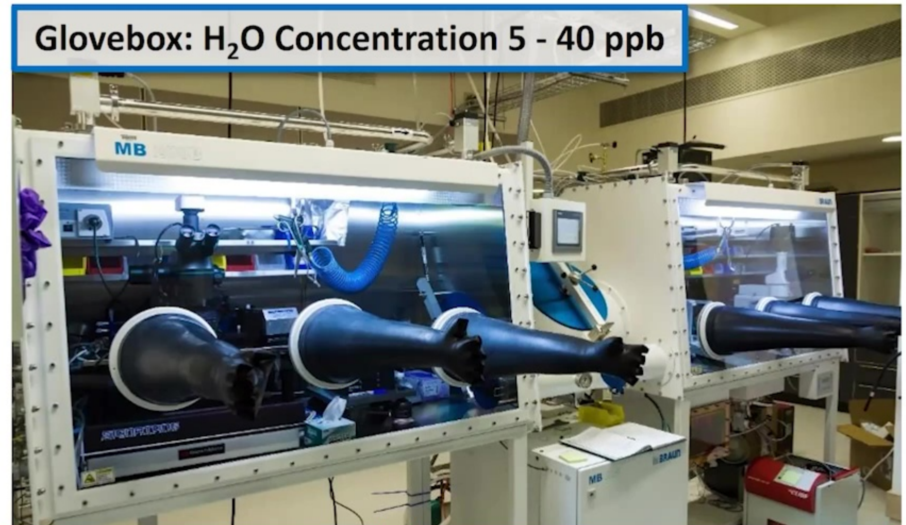

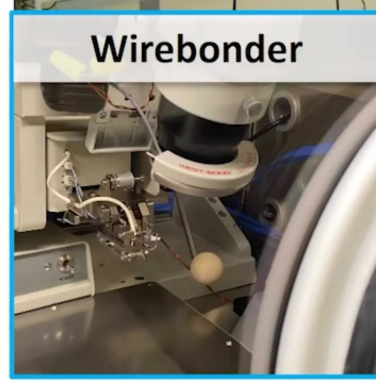

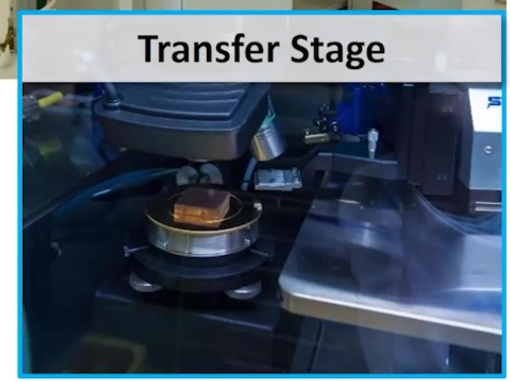

Stencil Mask Lithography

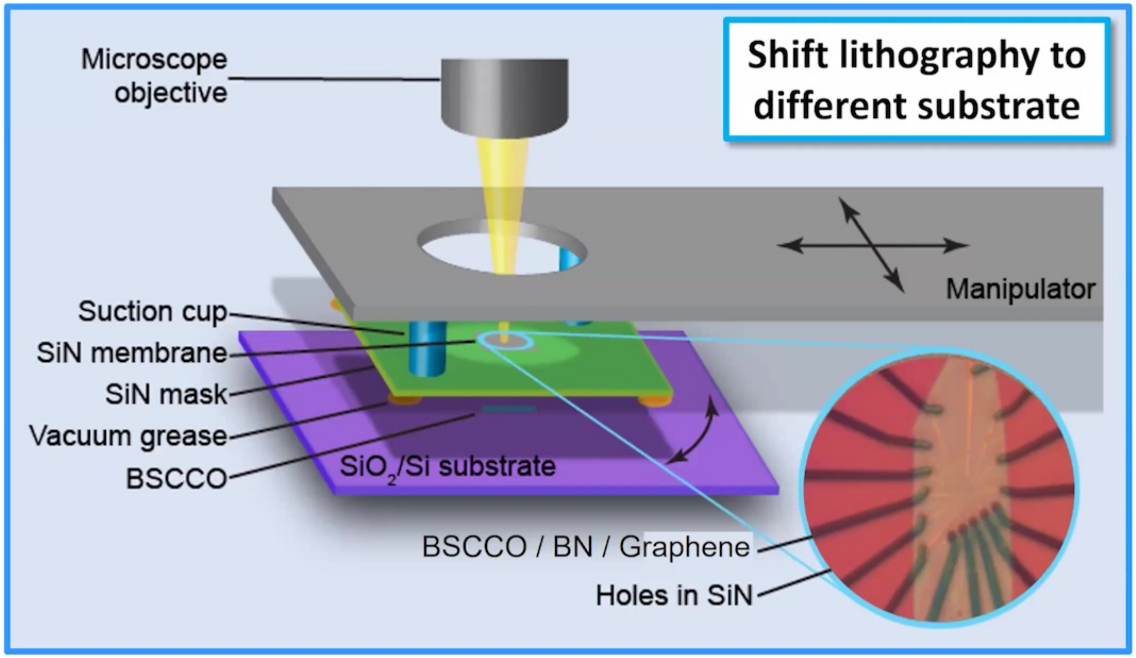

Stencil Mask Lithography

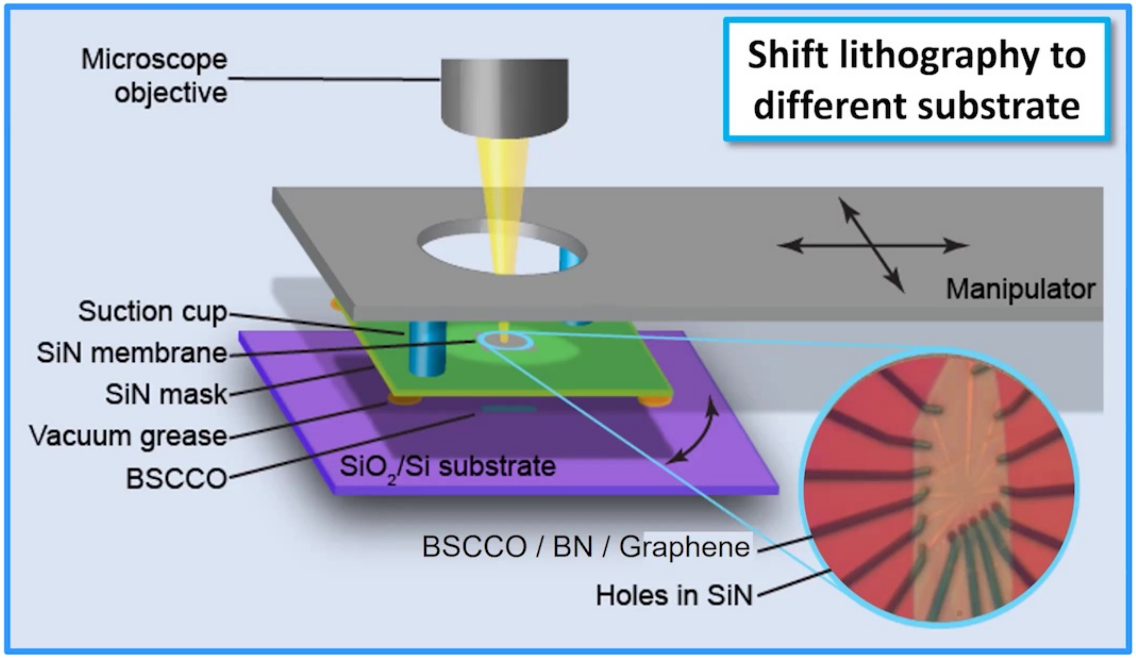

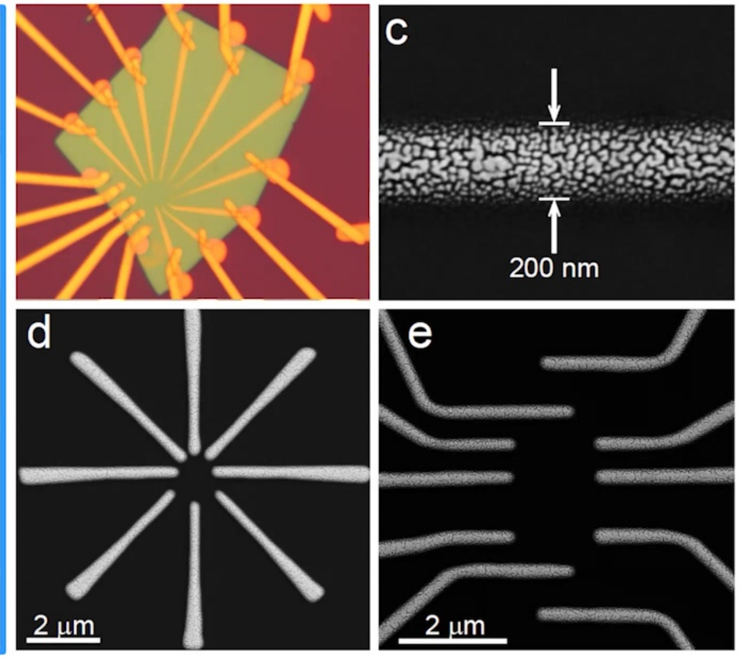

Technique advantages:
No air exposure
No heating
No solvent, no residue.

Technique capabilities

Resolution:	< 200 nm
Alignment:	< 1μm

Ultra-Clean twisted BSCCO Interface

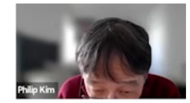

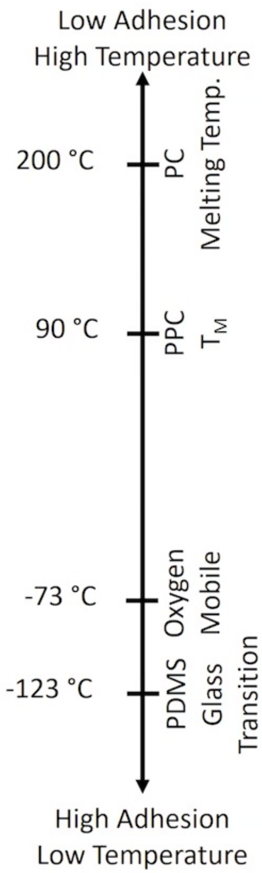

Stacking: Cryogenic PDMS Pickup

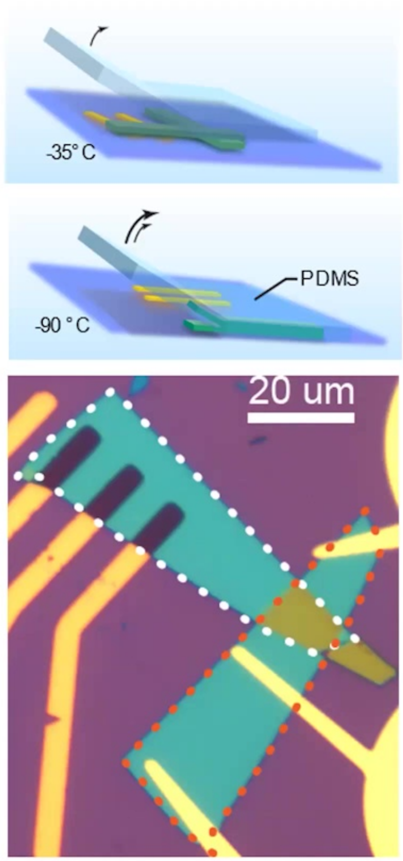

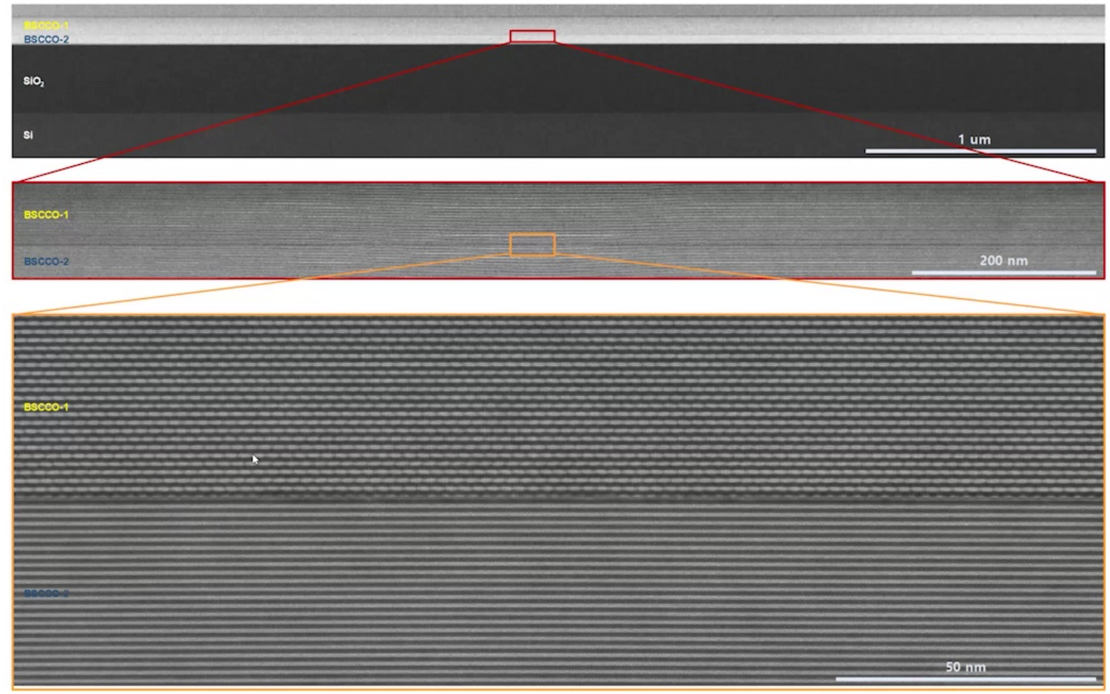

Ultra-Clean twisted BSCCO Interface

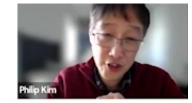

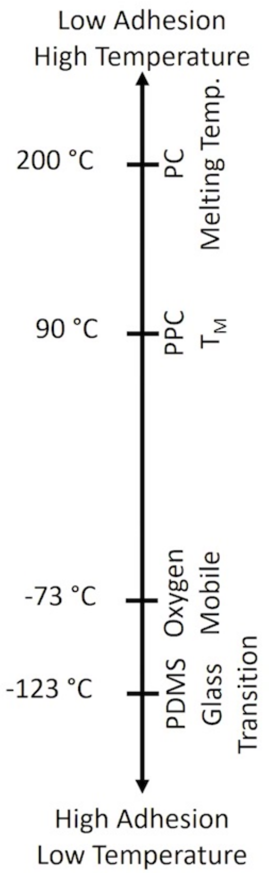

Stacking: Cryogenic PDMS Pickup

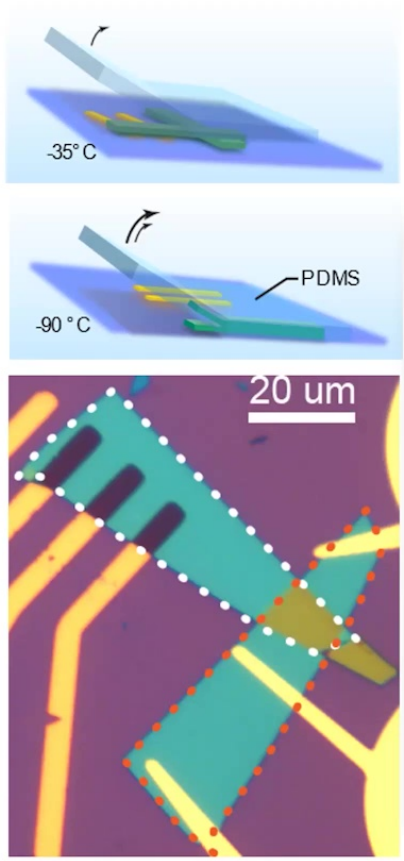

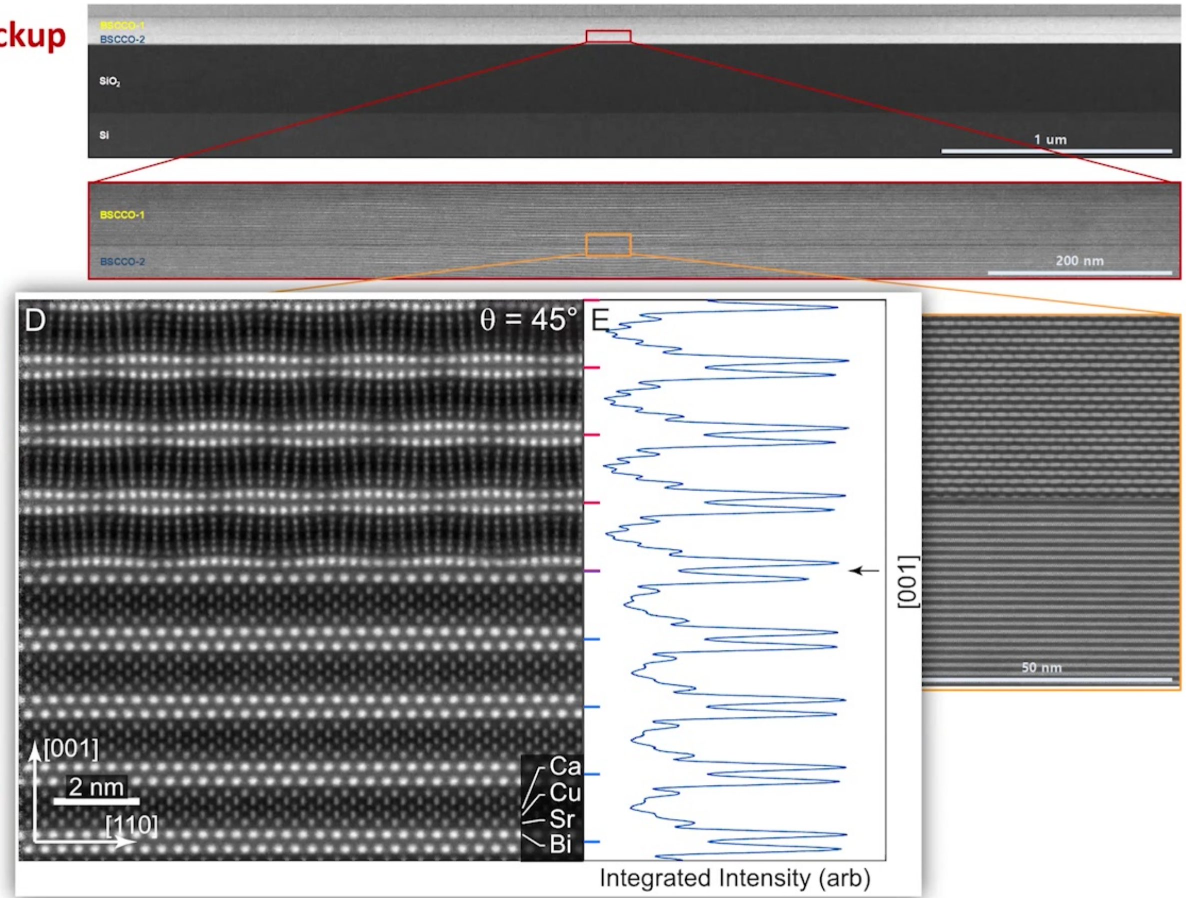

Artificial Vertical Josephson Junction Characteristics

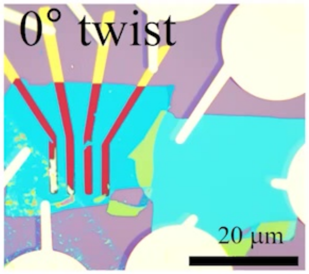

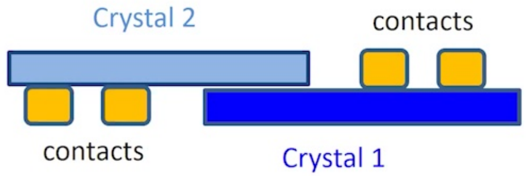

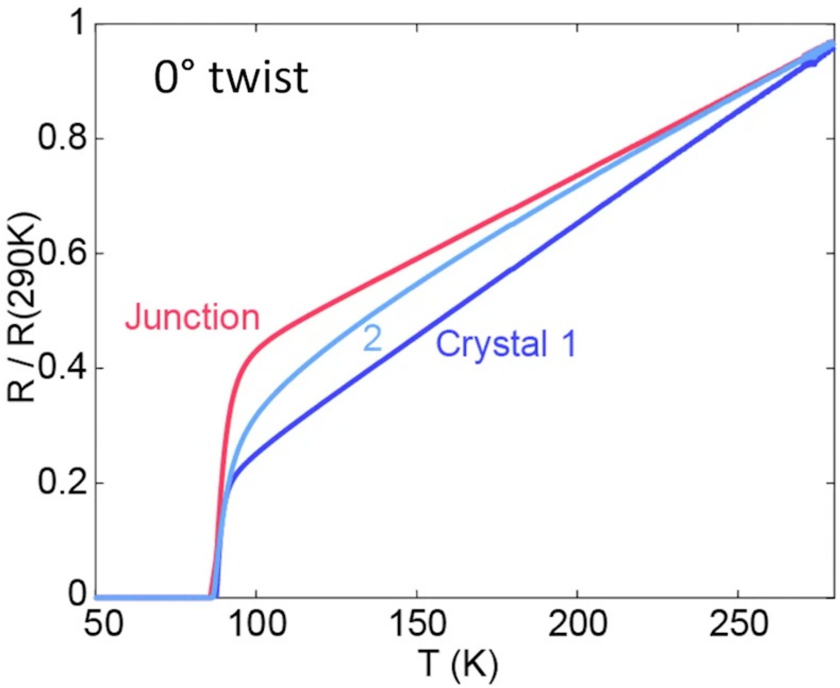

Josephson Junction Characteristics: 0° twist

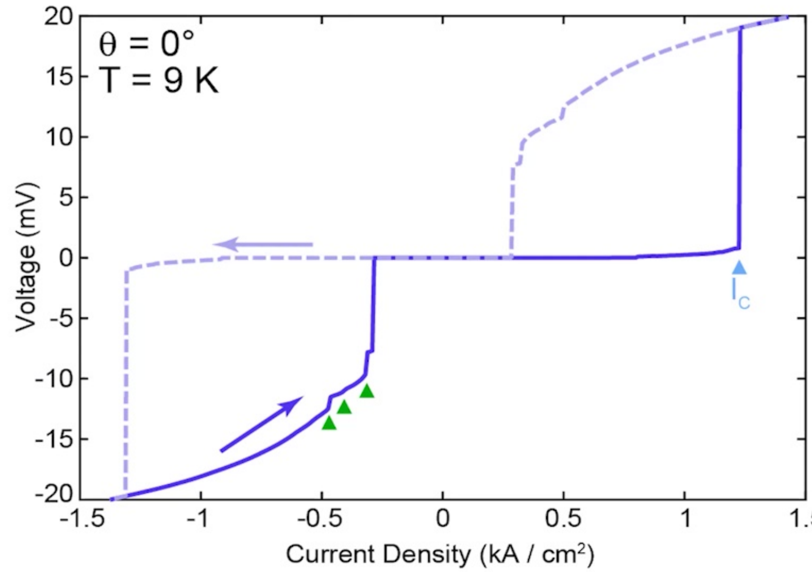

Critical switching current density is smaller than but comparable to intrinsic BSCCO JJ.

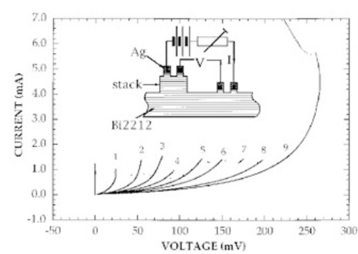

BSCCO intrinsic Junction
Junction Area ~1000 μm^2

Yurgens et. al., PRB 53 R8887 (1996)

Artificial Vertical Josephson Junction Characteristics

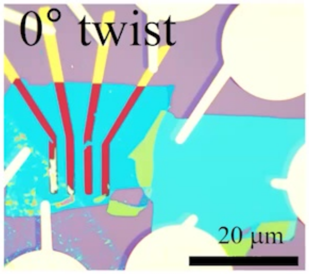

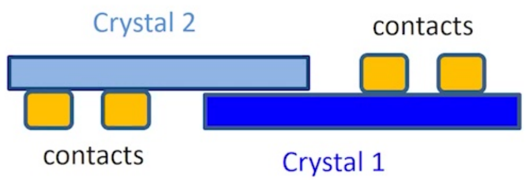

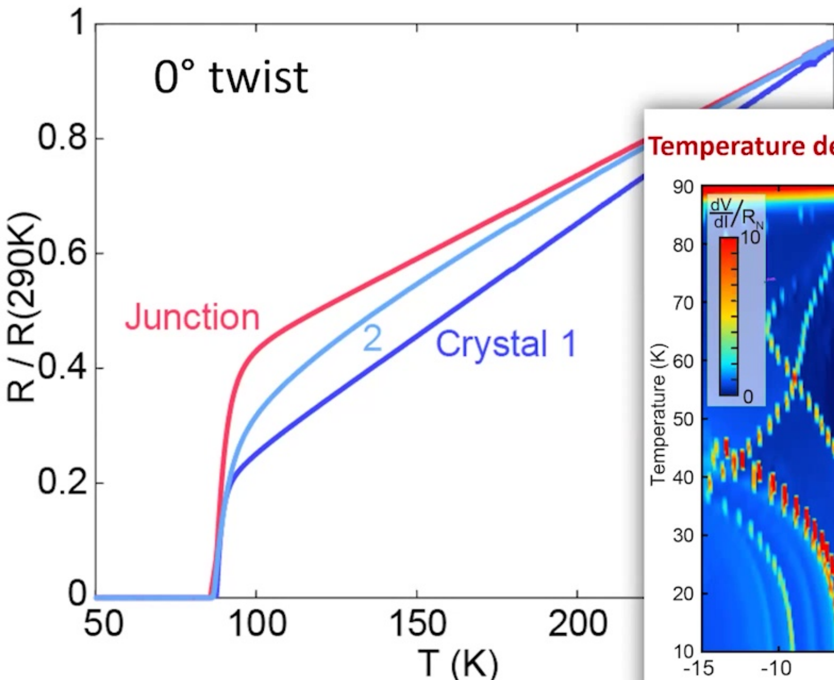

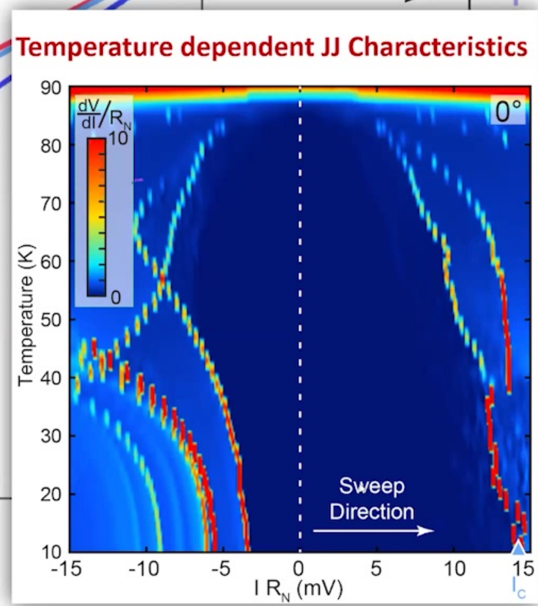

Josephson Junction Characteristics: 0° twist

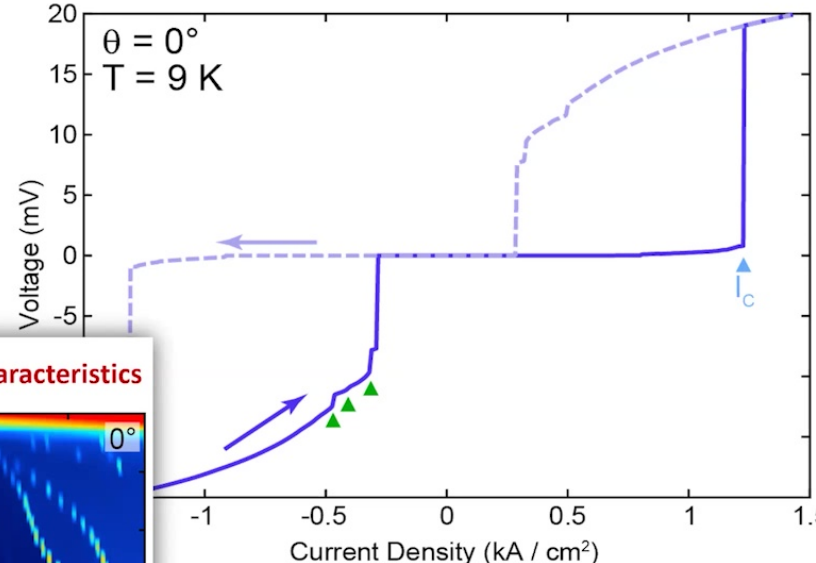

Critical switching current density is smaller than but comparable to intrinsic BSCCO JJ.

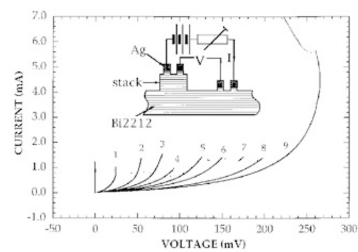

BSCCO intrinsic Junction
Junction Area ~1000 μm^2

Yurgens et. al., PRB 53 R8887 (1996)

Twisted BSCCO vdW Josephson Junctions

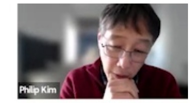

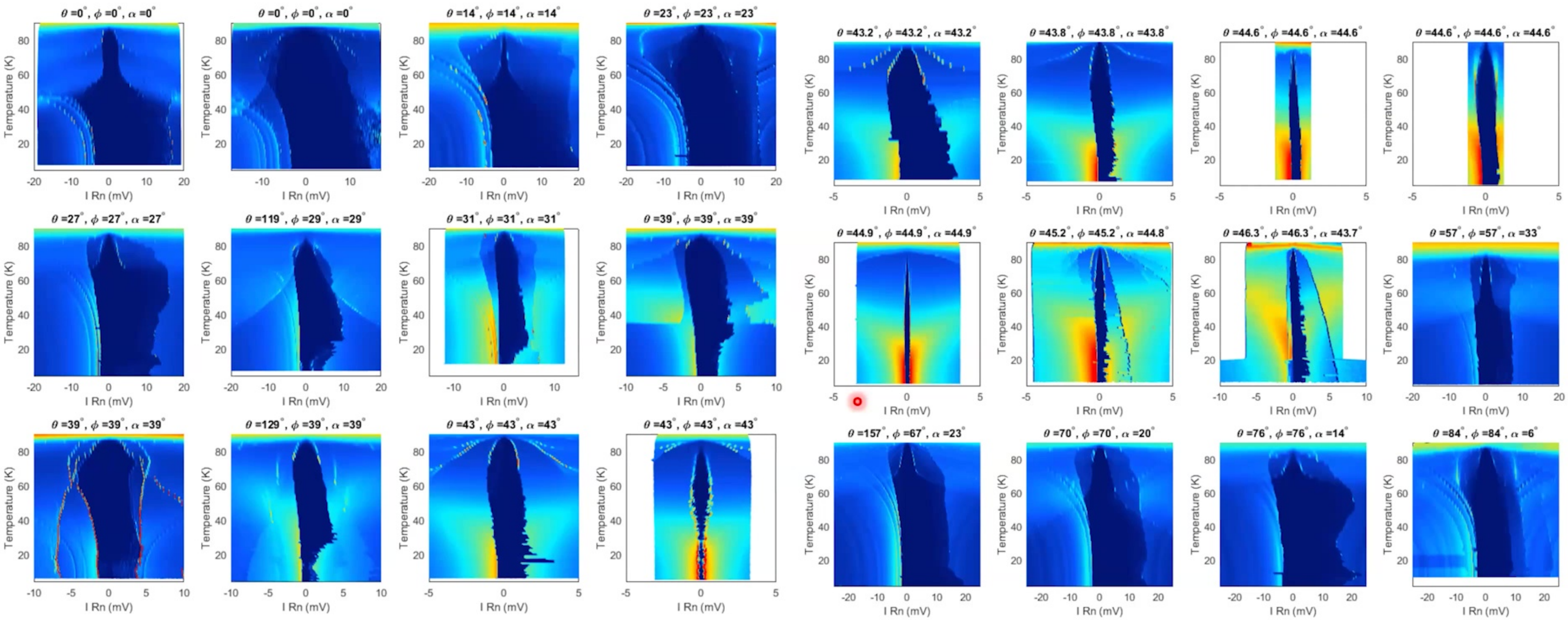

More than 24 junctions (so far): θ ranges 0° to 180°

Twisted BSCCO vdW Josephson Junctions

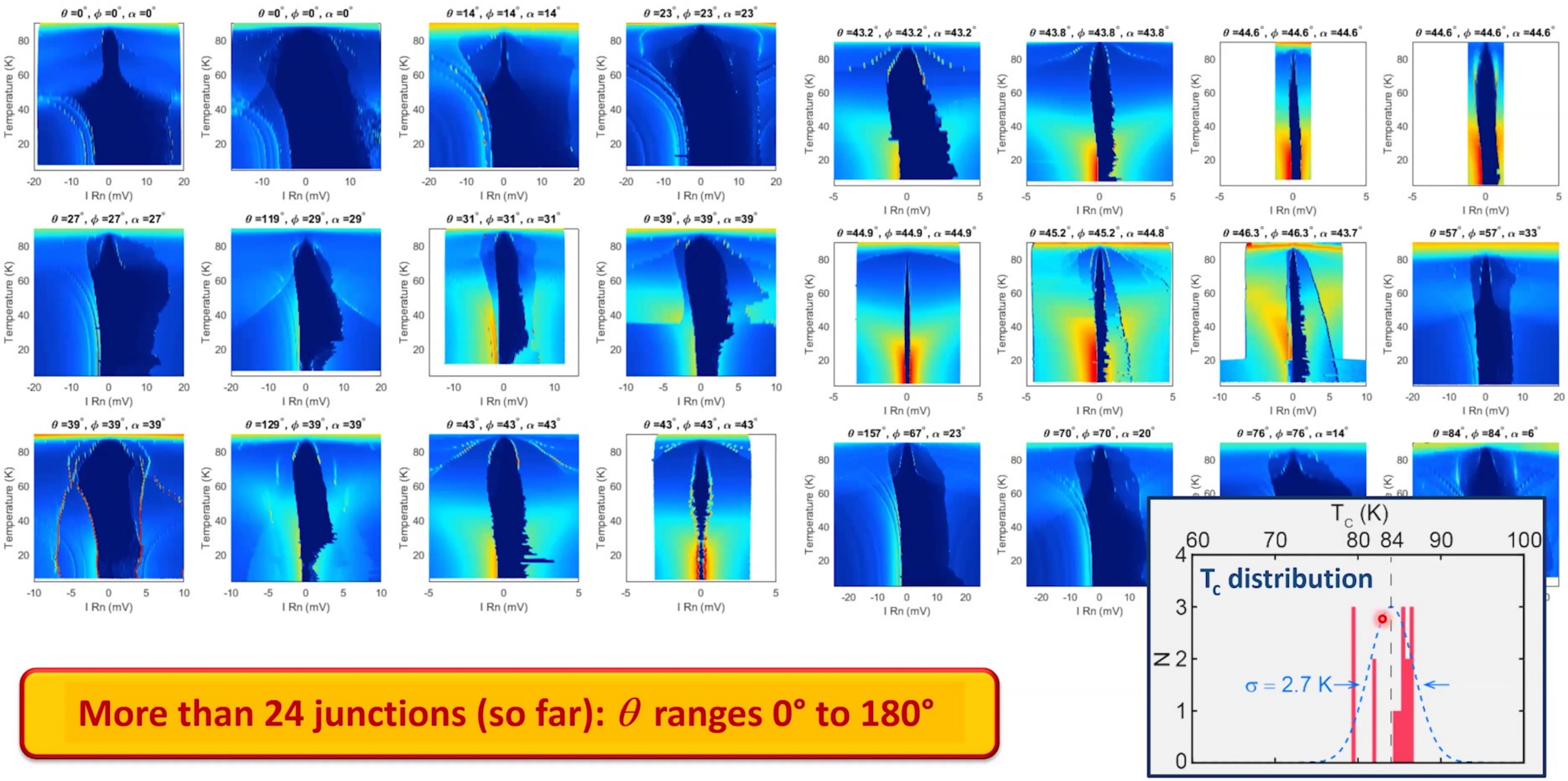

More than 24 junctions (so far): θ ranges 0° to 180°

Twisting Angle Dependence I_cR_N

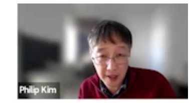

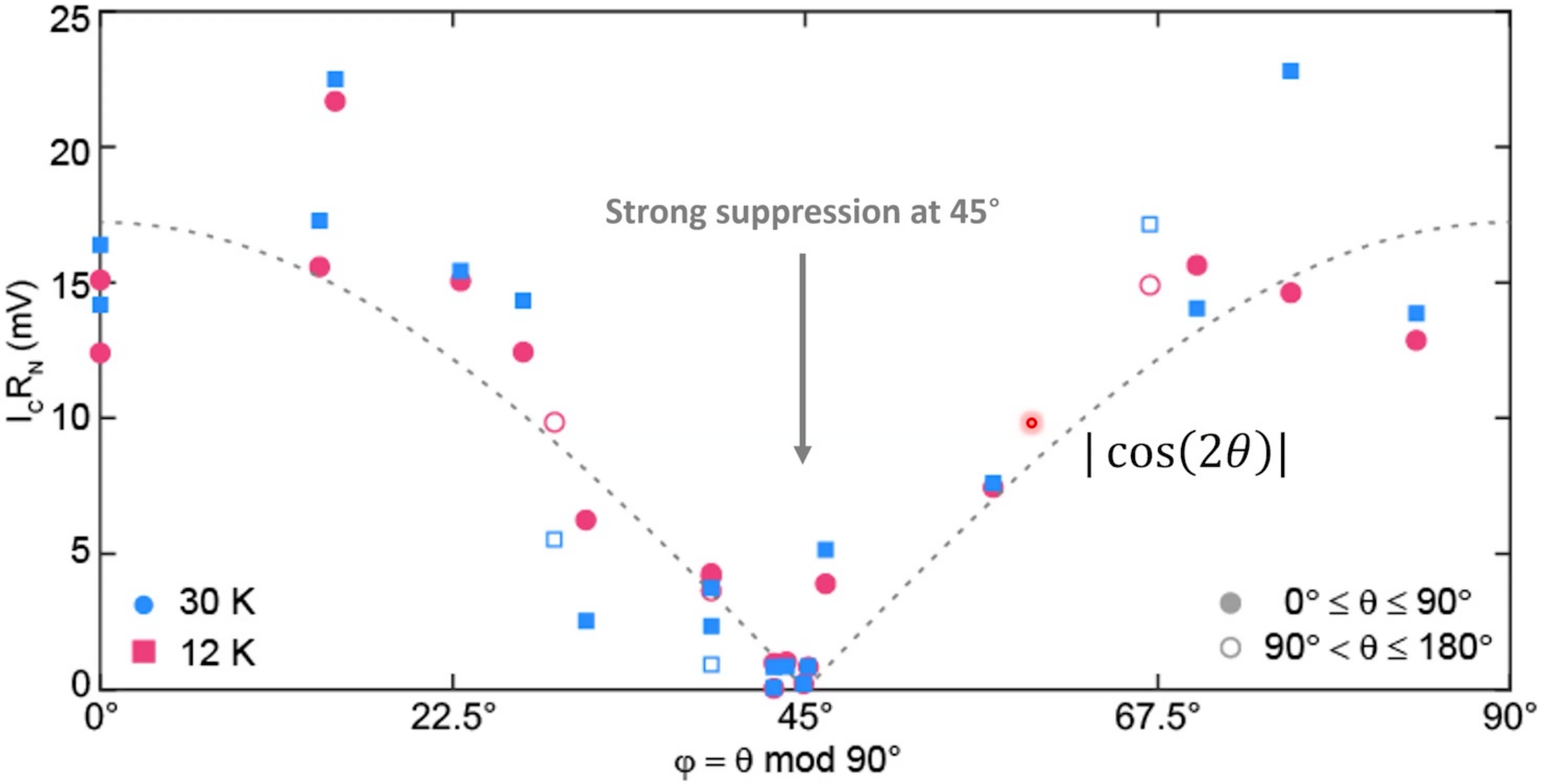

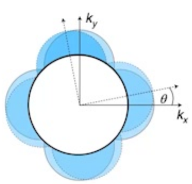

$$\Delta_{k1} = \Delta\cos(2\alpha_k + \theta), \quad \Delta_{k2} = \Delta\cos(2\alpha_k - \theta)$$

Twisted d-wave order parameters

Temperature Dependent Critical Current

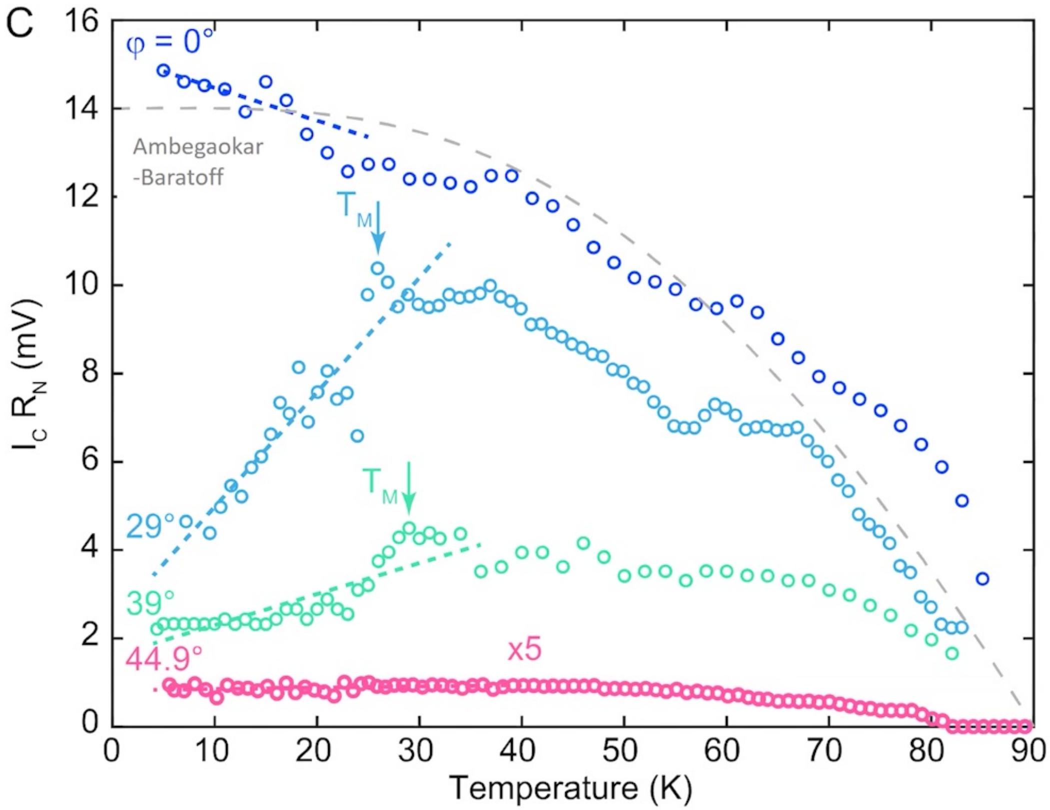

Non-monotonic temperature dependent I_c

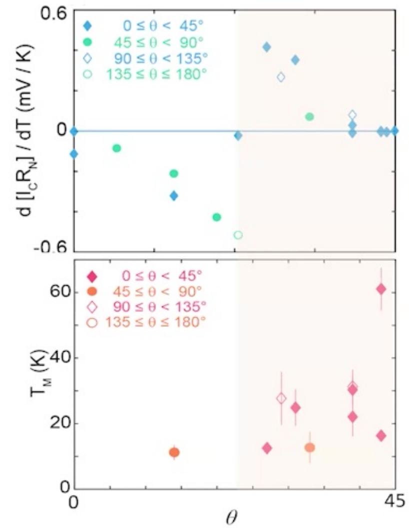

$0 \le \theta \lesssim \pi/8$

Decreasing I_c with increasing T

$\pi/8 \lesssim \theta \lesssim \pi/4$

Increasing I_c with increasing T at low temperature (non-monotonic)

$\theta \approx \pi/4$

Suppressed (but finite) I_c

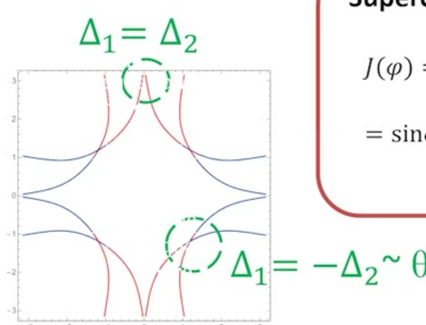

Supercurrent

$$J(\varphi) = \frac{2e}{\hbar}\frac{\partial \mathcal{F}(\varphi)}{\partial \varphi} = \sin\varphi \, \frac{eg^2}{\hbar} \sum_k \Delta_{k1}\Delta_{k2} \sum_{a=\pm} \frac{\operatorname{atanh}(E_{ka}/2k_BT)}{E_{ka}(E_{k-}^2 - E_{k+}^2)}$$

> 0

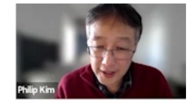

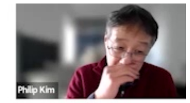

Temperature Dependent Critical Current

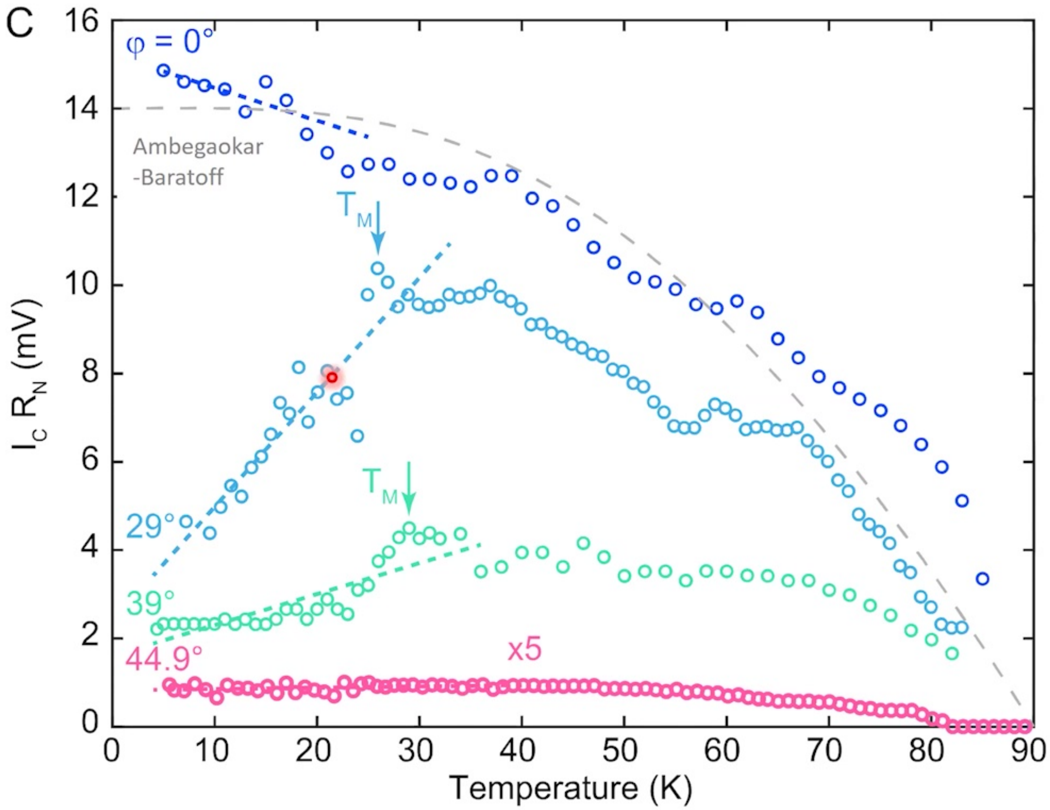

Non-monotonic temperature dependent I_c

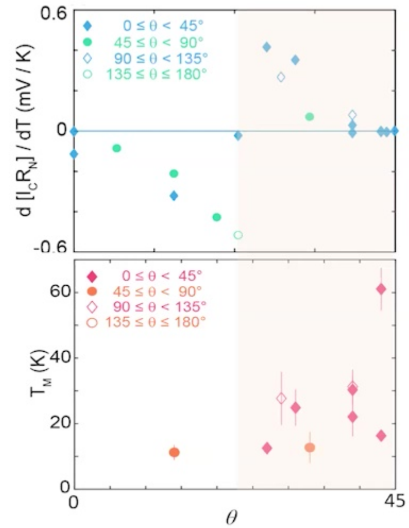

$0 \leq \theta \lesssim \pi/8$

Decreasing I_c with increasing T

$\pi/8 \lesssim \theta \lesssim \pi/4$

Increasing I_c with increasing T at low temperature (non-monotonic)

$\theta \approx \pi/4$

Suppressed (but finite) I_c

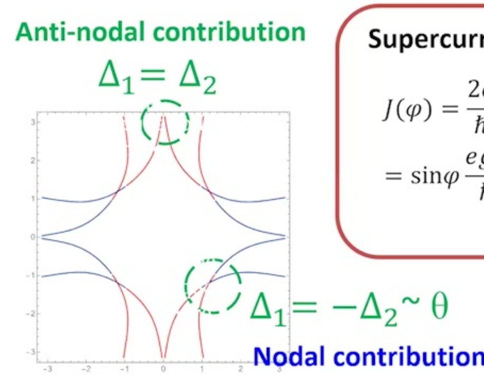

Supercurrent

$$J(\varphi) = \frac{2e}{\hbar}\frac{\partial \mathcal{F}(\varphi)}{\partial \varphi}$$

$$= \sin\varphi \, \frac{eg^2}{\hbar} \sum_k \Delta_{k1}\Delta_{k2} \sum_{a=\pm} \frac{\operatorname{atanh}(E_{ka}/2k_BT)}{E_{ka}(E_{k-}^2 - E_{k+}^2)}$$

> 0

Competing nodal and anti-nodal supercurrent contributions!

Near 45° Twisted Josephson Junctions

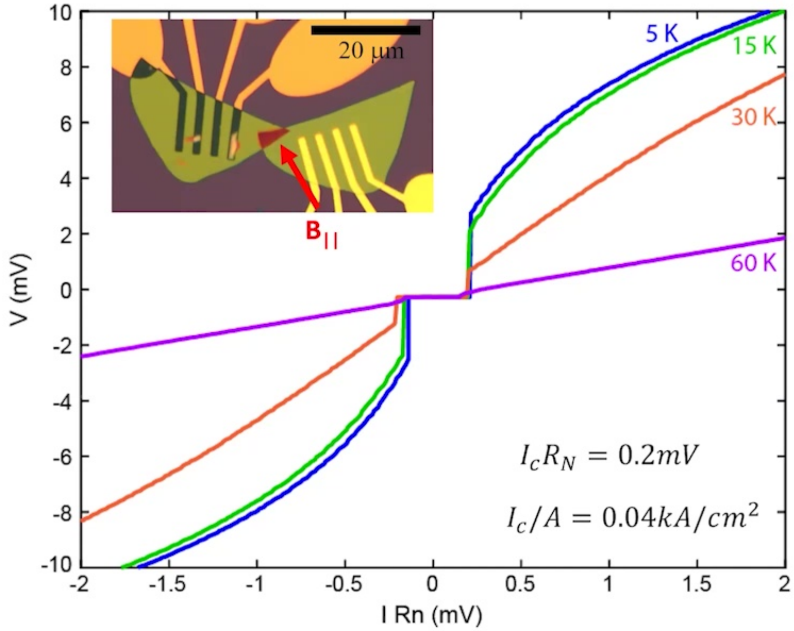

Reduced (~0.1 times of 0-twist), but finite I_cR_N

Temperature Dependent Critical Current

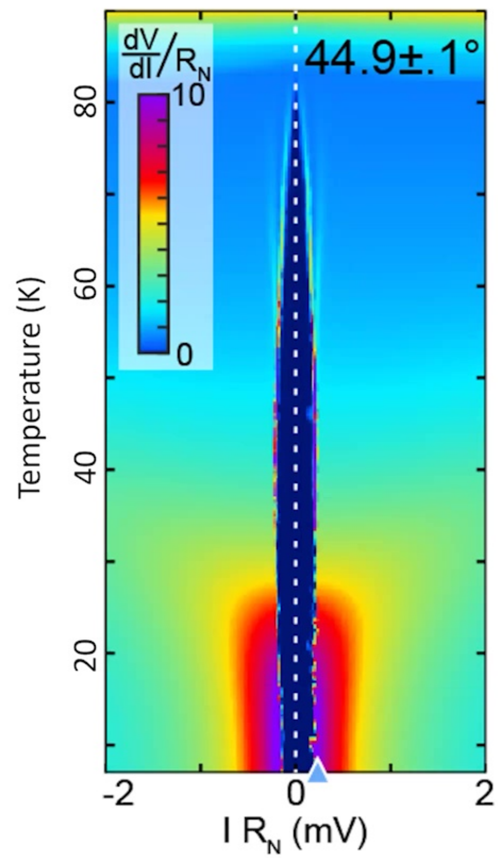

Fraunhofer Pattern with in-plane magnetic field

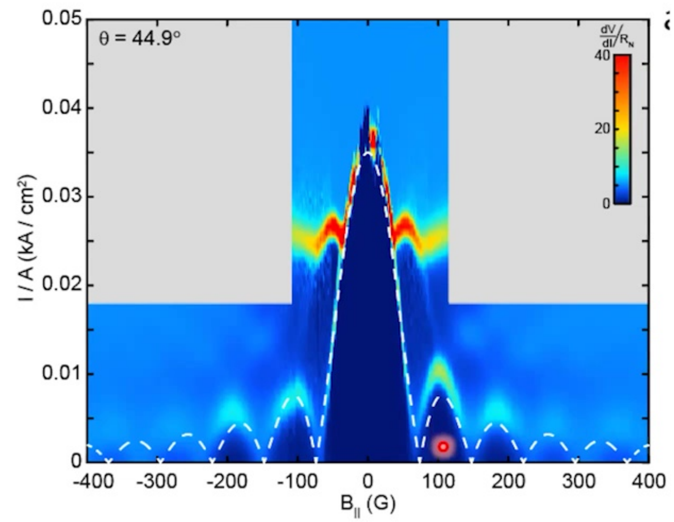

Well developed FP patterns suggest high quality Josephson Junction.

Fitting function: $I_C = I_{C0}\left|\frac{\sin\left(\frac{\pi\phi}{\phi_0}\right)}{\frac{\pi\phi}{\phi_0}}\right|$

$\phi = Bwt; \quad \phi_0 = 2.0678 \times 10^{-15}\ Tm^2$

Width: 11 μm (measured)

Fitting Parameters: **Thickness: 27 nm**

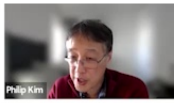

Fraunhofer Patterns in Twisted BSCCO Josephson Junction

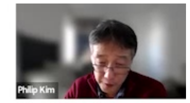

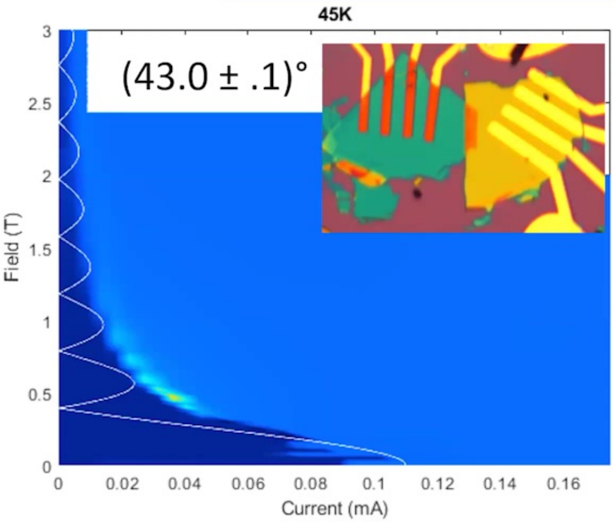

Fitting Parameters: Width: 3.5 μm
Thickness: 1.5 nm

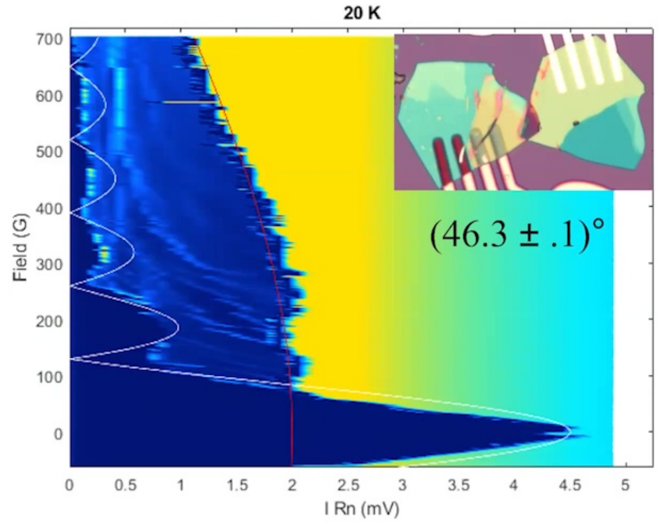

Fitting Parameters: Width: 11 μm
Thickness: 14.5 / 1.5 nm

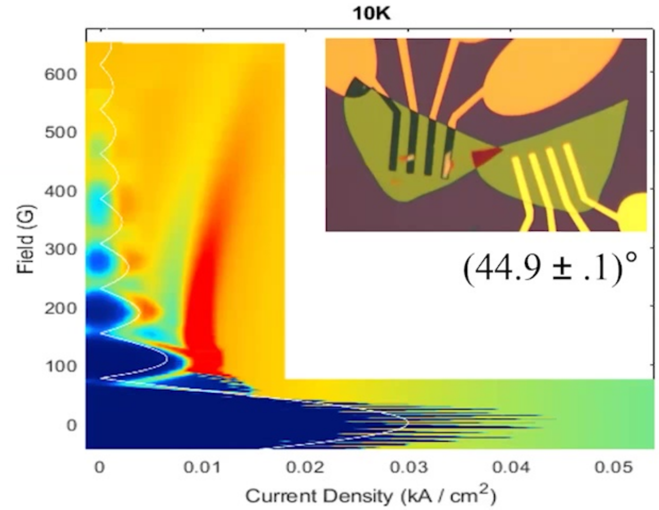

Fitting Parameters: Width: 10 μm
Thickness: 27 nm

Intrinsic BSCCO Josephson Junction

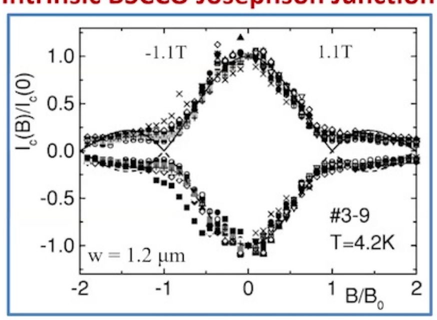

Irie et al, Phys. Rev. B 62 6681

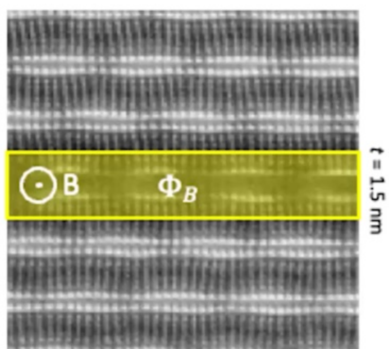

Bulaevskii, Clem & Glazman, Phys. Rev. B 46, 350

Two different Josephson current contributions

$$\mathcal{F}(\varphi) = \mathcal{F}_0 + 2B_0\psi^2[-\cos(2\theta)\cos\varphi + \mathcal{K}\cos(2\varphi)]$$

Shapiro Steps Measurement for JJ Current-Phase Relations

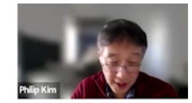

Microwave irradiation

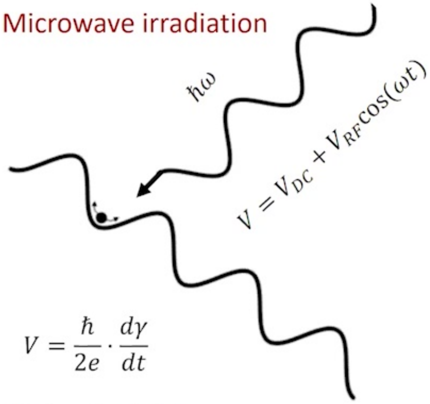

$$V = \frac{\hbar}{2e}\cdot\frac{d\gamma}{dt}$$

$$I(\gamma) = I_C \sin(\gamma)$$

Integer Shapiro steps

$n = 1, 2, 3, \dots$

$$V_{DC} = \frac{n\,\hbar}{2e}\cdot w_{RF}$$

$$I(\gamma) = I_C \sum_n (-1)^n J_n\left(\frac{2eV_{RF}}{\hbar\omega}\right)\sin\left(\gamma_0 + \frac{2eV_{DC}}{\hbar}t - n\omega_{RF}t\right)$$

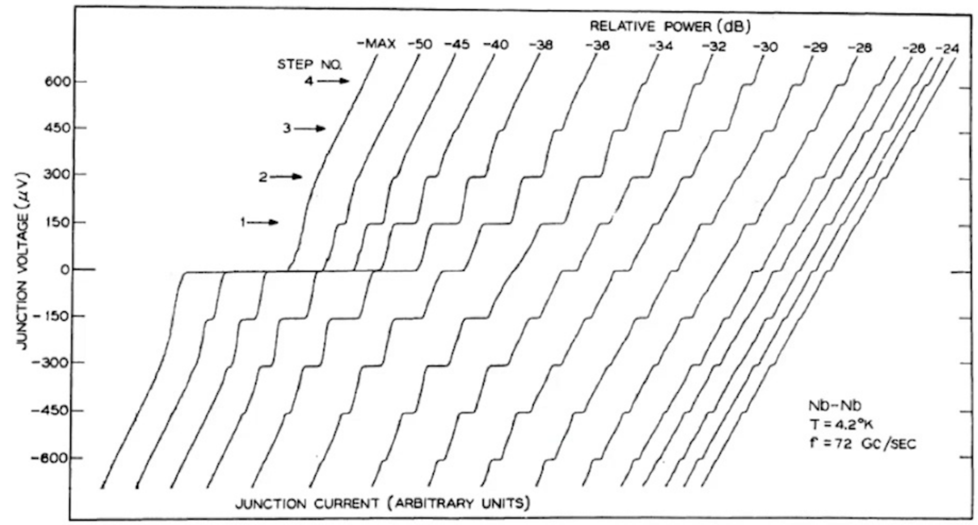

FIG. 1. Voltage-current curves for a Nb-Nb point-contact Josephson junction exposed to a 72-Gc/sec signal at various power levels.

Grimes and Shapiro Phys. Rev. (1967)

Fractional Josephson Effect: TI + Superconductors

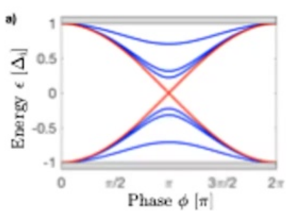

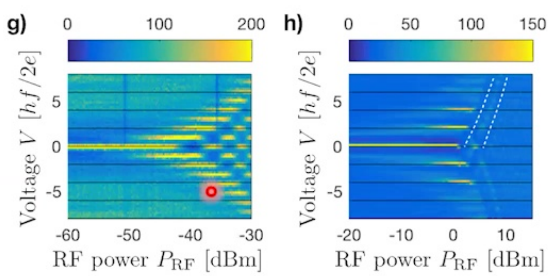

Bocquillon et al., arXiv:1810.03862

Shapiro Steps Measurement for JJ Current-Phase Relations

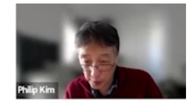

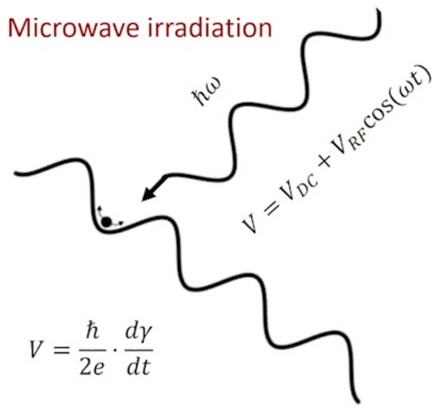

$$V = \frac{\hbar}{2e} \cdot \frac{d\gamma}{dt}$$

$$I(\gamma) = I_C \sin(\gamma)$$

Integer Shapiro steps

$n = 1, 2, 3, \ldots$

$$V_{DC} = \frac{n\,\hbar}{2e} \cdot w_{RF}$$

$$I(\gamma) = I_C \sum_n (-1)^n J_n\left(\frac{2eV_{RF}}{\hbar\omega}\right) \sin\left(\gamma_0 + \cancel{\frac{2eV_{DC}}{\hbar} t - n\omega_{RF} t}\right)$$

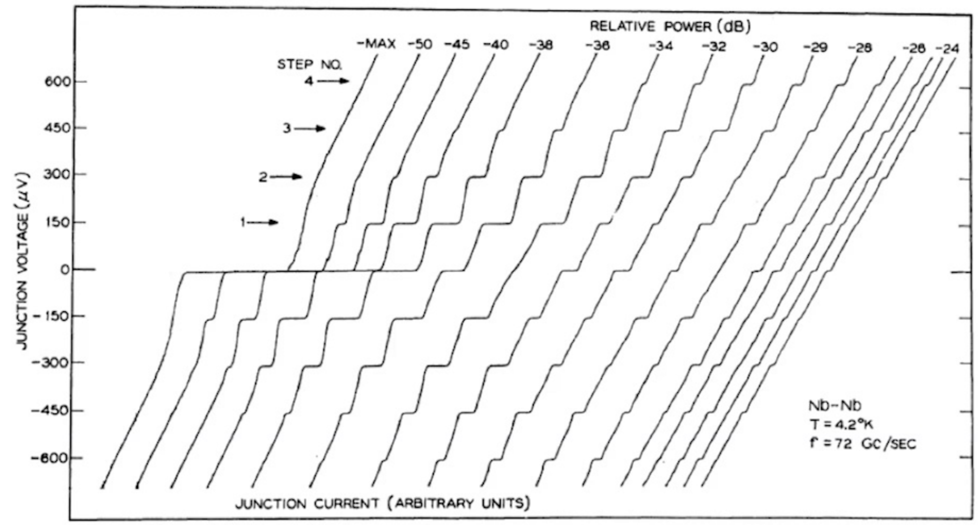

FIG. 1. Voltage-current curves for a Nb-Nb point-contact Josephson junction exposed to a 72-Gc/sec signal at various power levels.

Grimes and Shapiro Phys. Rev. (1967)

Fractional Josephson Effect: TI + Superconductors

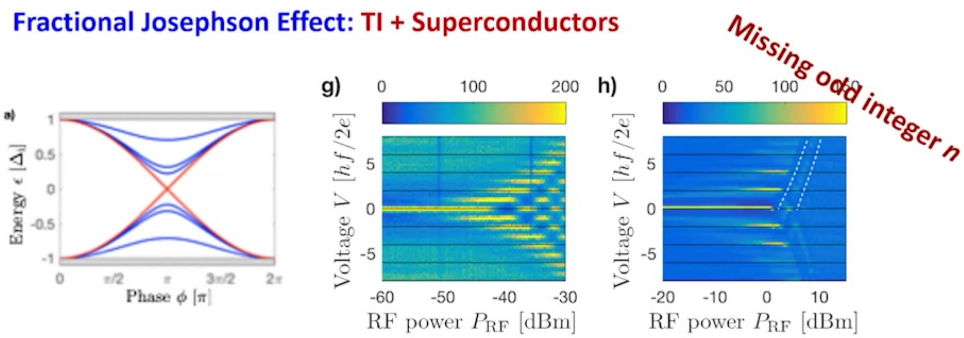

Bocquillon et al., arXiv:1810.03862

Fractional Shapiro Steps: phase slip CPR in superconducting nanowire

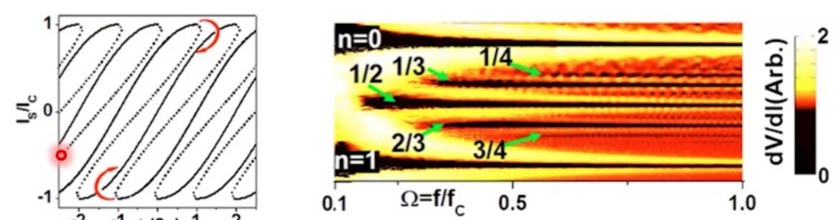

Dinsmore et al., APL 93, 192505 (2008)

Fractional Shapiro Steps: Presence of Second Harmonic Mode

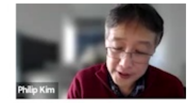

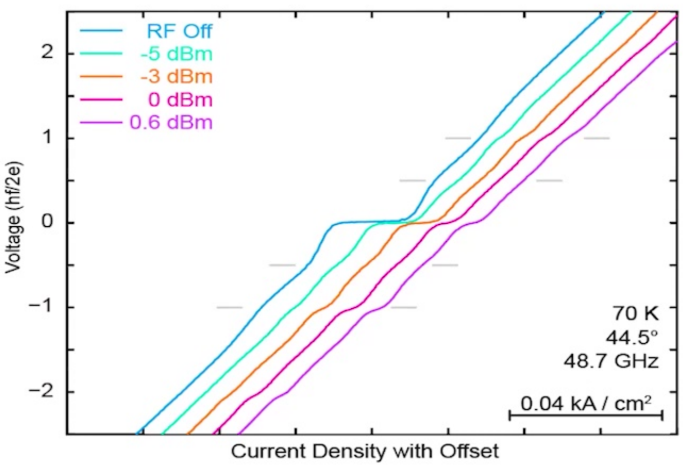

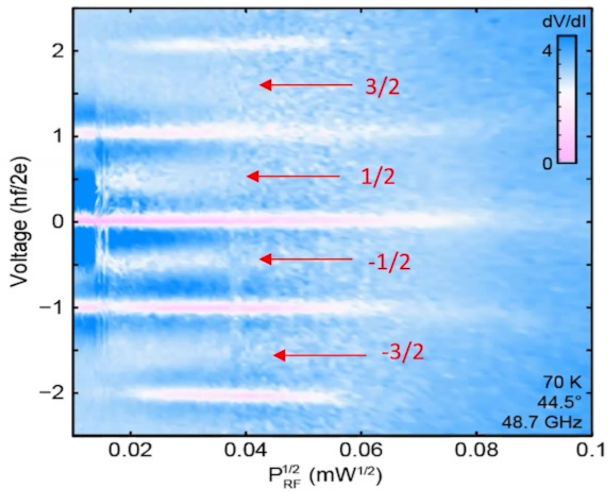

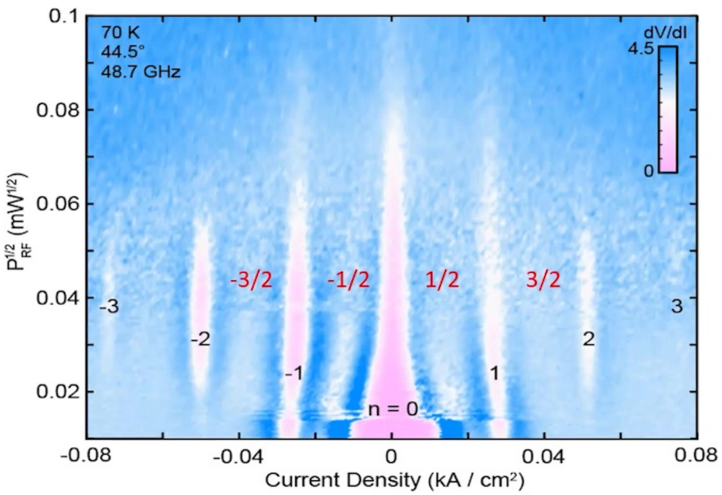

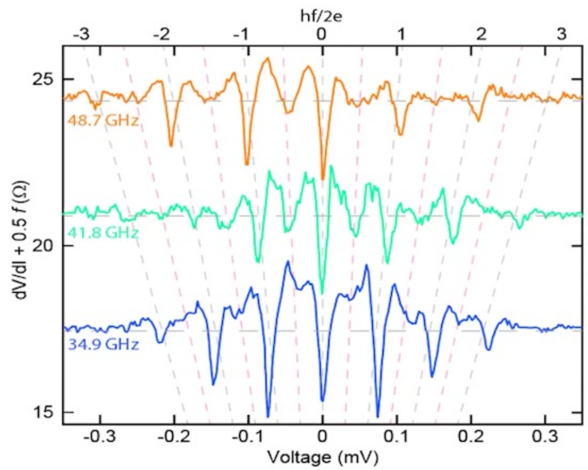

Can et al. Nature Phys (2021)

$$\mathcal{F}(\varphi) = \mathcal{F}_0 + 2B_0\psi^2[-\cos(2\theta)\cos\varphi + \mathcal{K}\cos(2\varphi)]$$

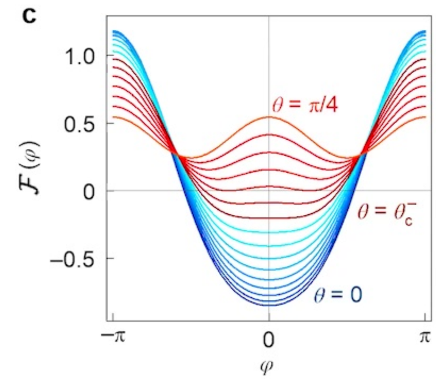

JJ current phase relation

$$J(\varphi) = \frac{2e}{\hbar}\frac{\partial \mathcal{F}(\varphi)}{\partial \varphi}$$

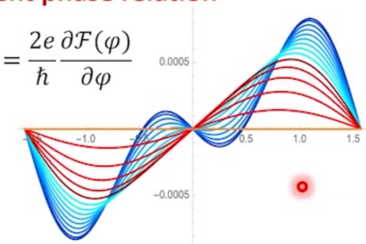

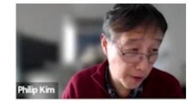

Fractional Shapiro Steps: Presence of Second Harmonic Mode

(43.7 ± .1)°

Integer Shapiro steps

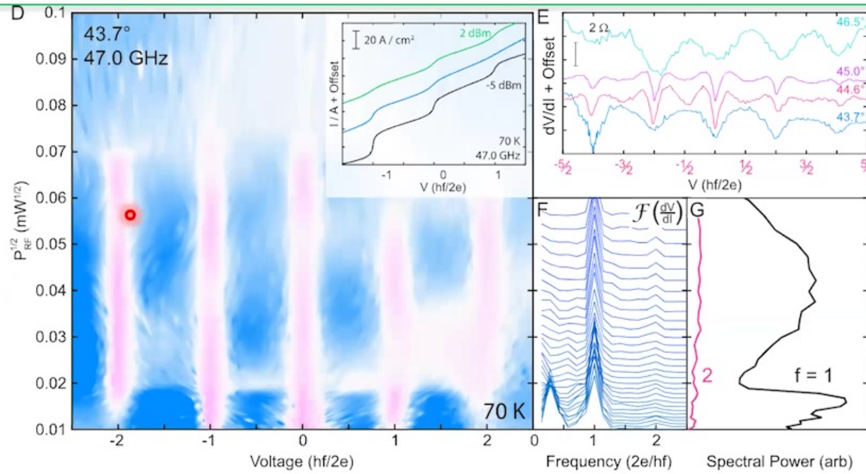

(44.6 ± .1)°

Dominant half Integer Shapiro steps

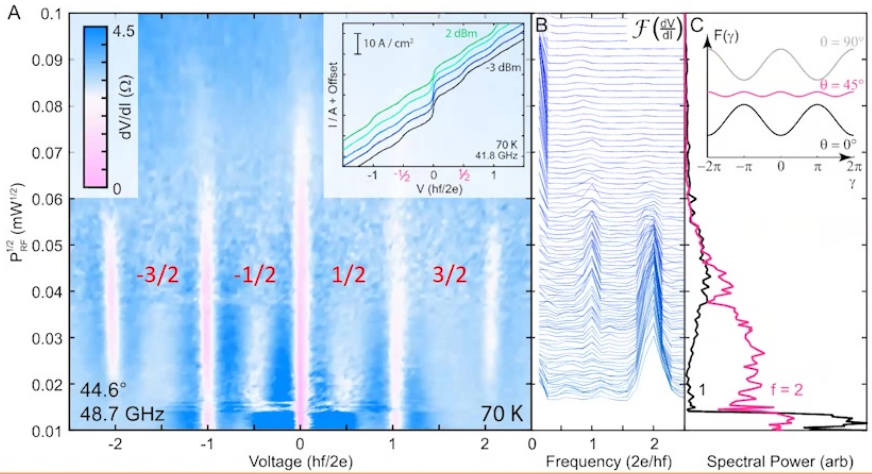

Can et al. Nature Phys (2021)

$$\mathcal{F}(\varphi) = \mathcal{F}_0 + 2B_0\psi^2[-\cos(2\theta)\cos\varphi + \mathcal{K}\cos(2\varphi)]$$

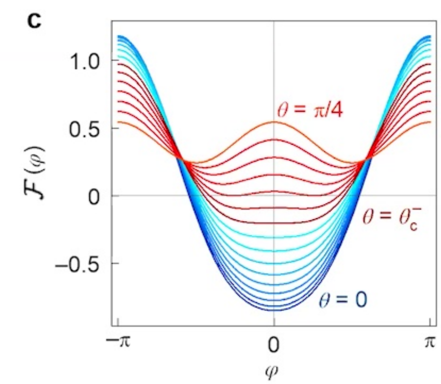

JJ current phase relation

$$J(\varphi) = \frac{2e}{\hbar}\frac{\partial \mathcal{F}(\varphi)}{\partial \varphi}$$

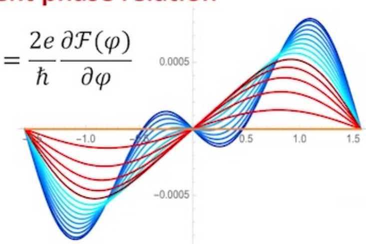

Observed fractional Shapiro steps suggest the presence of the second harmonic term!

Summary

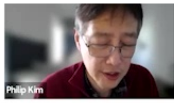

Twist Josephson Junctions Fabrication

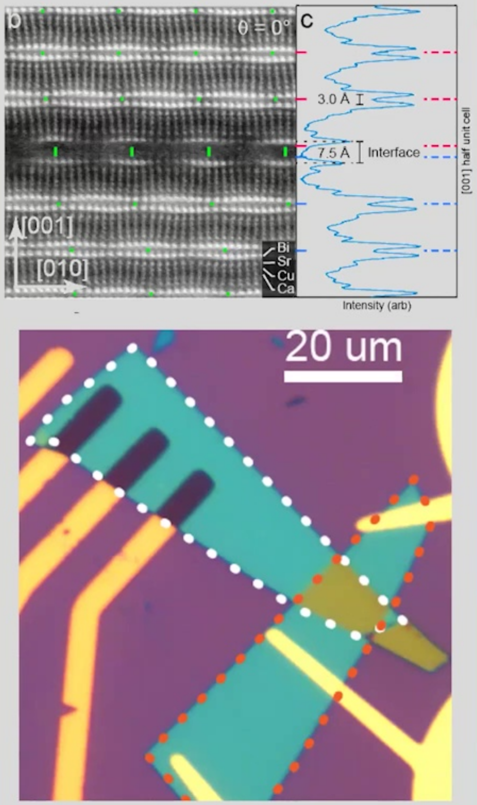

Twist Angle Dependent Critical Current

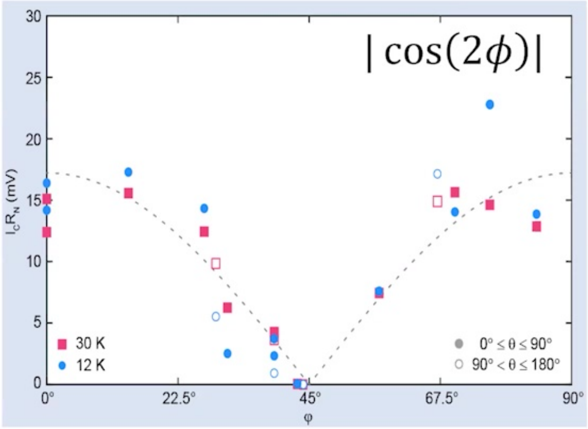

Unusual temperature dependent Ic

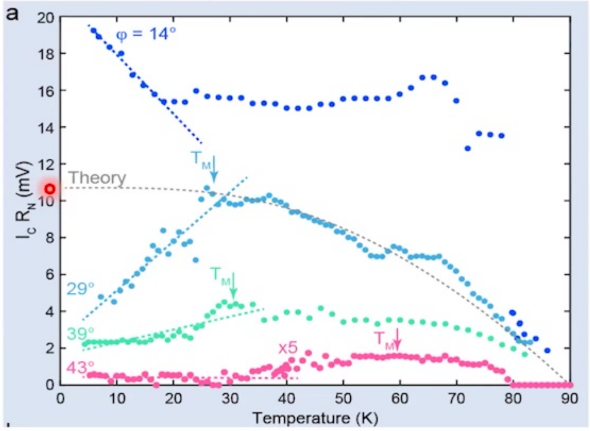

Fraunhofer pattern

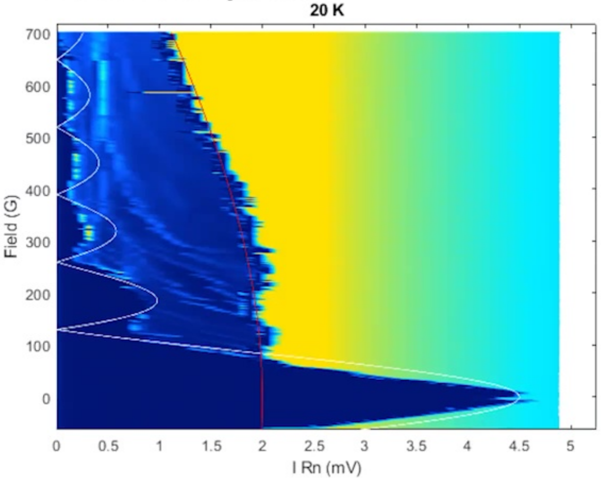

Fractional Shapiro Steps

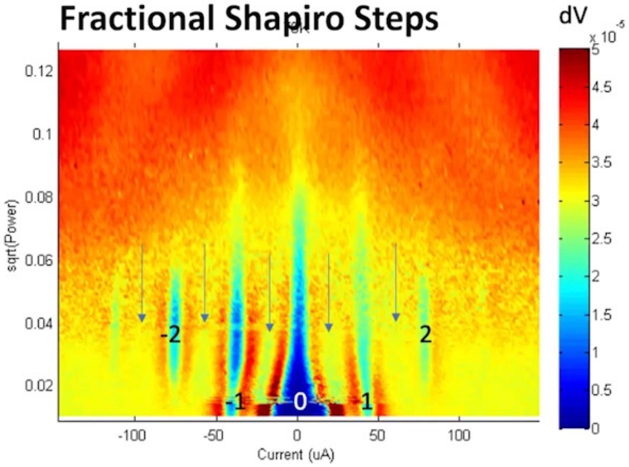

Outlook

Can we directly probe TSC with broken TRS?

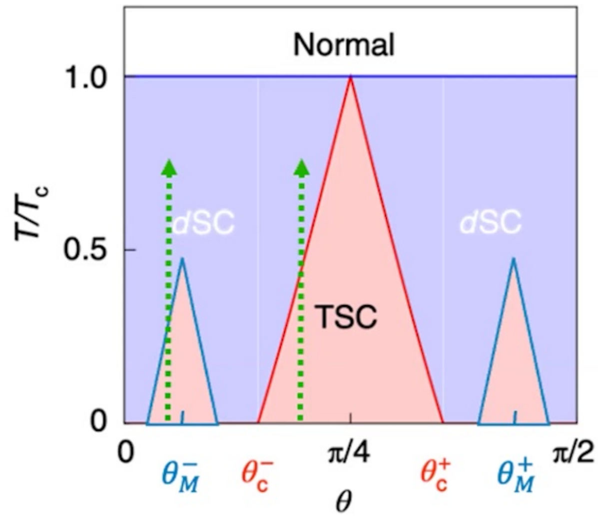

Can et al. Nature Phys (2021); Volkov et al. arXiv: 2012.07860

- Phase sensitive measurement: SQUID

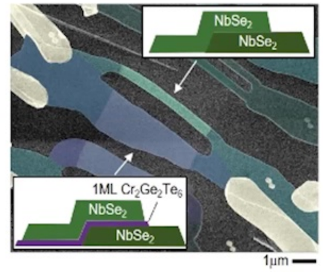

NbSe2: s-wave Ising SC
Cr2Ge2Te6: magnetic insulator
NbSe2: s-wave Ising SC

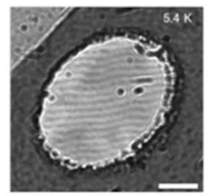

Magnetic domain structure of Cr2Ge2Te6

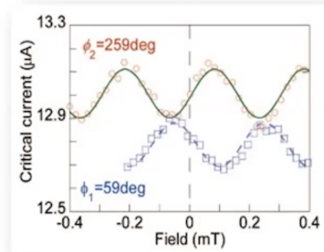

Idzuchi et al., Nature Comm. (2021)

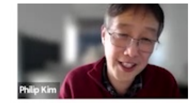

Outlook

Can we directly probe TSC with broken TRS?

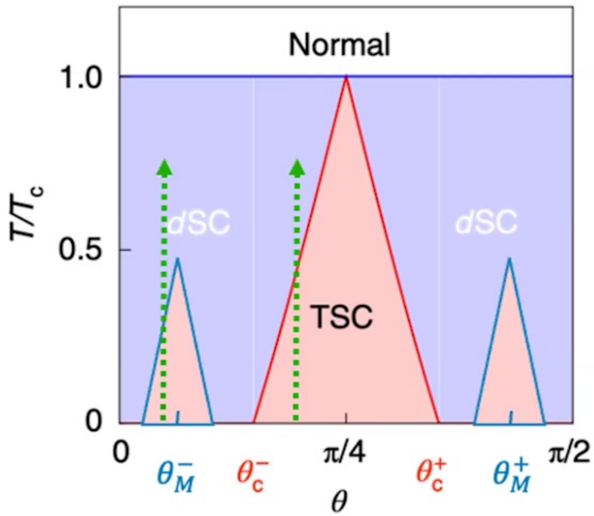

Can et al. Nature Phys (2021); Volkov et al. arXiv: 2012.07860

- Phase sensitive measurement: SQUID

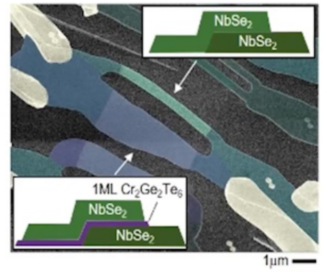

NbSe2: s-wave Ising SC
Cr2Ge2Te6: magnetic insulator
NbSe2: s-wave Ising SC

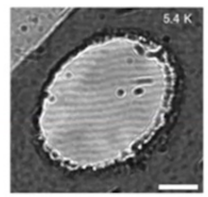

Magnetic domain structure of Cr2Ge2Te6

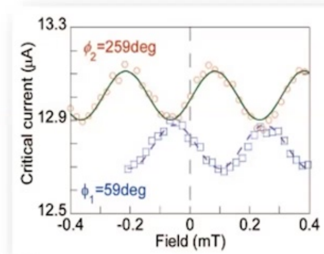

Idzuchi et al., Nature Comm. (2021)

- Edge state measurement: thermal transport

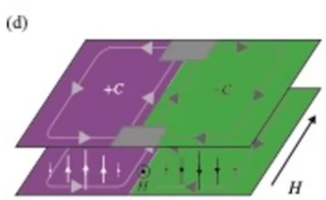

- Other means of broken TRS measurement: Kerr effect and etc

Acknowledgment

Experiment

Frank Zhao, Nicolar Poccia, Xiaomeng Cui, Hyobin Yoo, Joon Young Park, Yuval Ronen, Rebecca Engelke

Samples

Rudan Zhong, Genda Gu (BNL); Kenji Watanabe, Takashi Taniguchi (NIMS)

Theory

Pavel Volkov, Jed Pixley (Rutgers); Tarun Tummuru, Stephan Plugge, Marcel Franz (UBC)